Coupled mechanical mapping and interference contrast microscopy reveal viscoelastic and adhesion hallmarks of monocyte differentiation into macrophages

Mar Eroles, Javier Lopez-Alonso, Alexandre Ortega, Thomas Boudier, Khaldoun Gharzeddine, Frank Lafont, Clemens Franz, Arnaud Millet, Claire Valotteau, Felix Rico

Coupled mechanical mapping and interference contrast microscopy reveal viscoelastic and adhesion hallmarks of monocytes differentiation into macrophages

Mar Eroles[1], Javier Lopez-Alonso[2], Alexandre Ortega[1], Thomas Boudier[3], Khaldoun Gharzeddine[4-5], Frank Lafont[2], Clemens Martin Franz[6], Arnaud Millet[4-5], Claire Valotteau[1], Felix Rico[1].

[1] Aix-Marseille University, INSERM, CNRS, LAI (U1067), Turing Centre for Living Systems, Marseille, France.

[2] Univ. Lille, CNRS, Inserm, CHU Lille, Institut Pasteur Lille, U1019 - UMR 9017 - CIIL - Center for Infection and Immunity of Lille, Lille, France.

[3] Centuri, Turing Centre for Living Systems, Marseille, France.

[4] Univ.Grenoble Alpes, Inserm U1209, CNRS UMR5309, Institute for Advanced Biosciences, Team Mechanobiology, Immunity and Cancer, La Tronche, France.

[5] Department of Hepatogastroenterology, Centre Hospitalier Universitaire de Grenoble Alpes, La Tronche, France.

[6] WPI Nano Life Science Institute, Kanazawa University, Kanazawa, Japan.

Abstract

Monocytes activated by pro-inflammatory signals adhere to the vascular endothelium and migrate from the bloodstream to the tissue ultimately differentiating into macrophages. Cell mechanics and adhesion play a crucial role in macrophage functions. However, how monocytes change their adhesion and mechanical properties upon differentiation into macrophages is still not well understood. In this work, we used various tools to quantify the morphology, adhesion, and viscoelasticity during this process. Combination of atomic force microscopy (AFM) high resolution viscoelastic mapping with interference contrast microscopy (ICM) at the single-cell level revealed viscoelasticity and adhesion hallmarks during monocyte differentiation into macrophages. Quantitative holographic tomography imaging revealed a dramatic increase in cell volume and surface area during monocyte differentiation and the emergence of round and spread macrophage subpopulations. AFM viscoelastic mapping revealed important stiffening (increase of the apparent Young's modulus, E_0) and solidification (decrease of cell fluidity, β) on differentiated cells that correlated with increased adhesion area. These changes were enhanced in macrophages with a spread phenotype. Remarkably, when adhesion was perturbed, differentiated macrophages remained stiffer and more solid-like than monocytes, suggesting a permanent reorganization of the cytoskeleton. We speculate that the more solid-like microvilli and lamellipodia might help macrophages to minimize energy dissipation during mechanosensitive activities. Our results revealed viscoelastic and adhesion hallmarks of monocyte differentiation that may be important for biological function.

Keywords: cell mechanics, macrophages, viscoelasticity, atomic force microscopy, interference contrast microscopy, CD11b, holographic tomography.

Introduction

Monocytes are circulating cells patrolling the vascular endothelium in search of external agents or inflammatory signals(Ley and Fan 2018). During inflammation, monocytes become adherent, able to trespass the vascular endothelium and the tissue to reach the site of injury or infection (Vicente-Manzanares and Sánchez-Madrid 2004; Muller 2013). To overcome external dangers, such as viruses or bacteria infections, monocytes differentiate into macrophages. Macrophages are highly specialized cells with a high phagocytic activity that once activated will be crucial for the inflammatory response and tissue healing(Jain, Moeller, and Vogel 2019; Liu et al. 2016; Van den Bossche and Saraber 2018).

This process starts with the adhesion of the activated monocytes onto the vascular endothelium through specific interactions with adhesion molecules, like selectins and integrins (Ley and Fan 2018; de Fougerolles et al. 2000; Lamers, Plüss, and Ricklin 2021). After activation and firm adhesion, monocytes trespass the endothelium deforming its cytoskeleton, forming pseudopodia and exerting traction forces to pull its body through the extracellular matrix(Vicente-Manzanares and Sánchez-Madrid 2004; Hsieh et al. 2019). Finally, monocytes differentiate into macrophages that are able to phagocytize external agents and start secreting inflammation mediators (pro-inflammatory and anti-inflammatory), until the tissue is back to its homeostatic state(Medzhitov 2008; Stone, Basit, and Burns 2022).

Macrophage differentiation is a crucial process during the first steps of the immune response. Exposure of monocytes to phorbol ester activates the PKC pathway, which stops proliferation and starts differentiation to M0 macrophages(Homma, Henning-Chubb, and Huberman 1986; Chang et al. 2012). This differentiation process has been extensively studied but quantification of relevant features has been elusive(Schwende et al. 1996; Auwerx 1991; Kohro et al. 2004; Spano, Barni, and Sciola 2013; Starr et al. 2018). Biological changes like membrane antigens, secretory products (interleukins), and proto-oncogenes activation have been shown(Auwerx 1991; Rovera, O'Brien, and Diamond 1979). However, several morphological changes, like the increase in cell volume and cell diameter, have been difficult to quantify(Tsuchiya et al. 1982). During differentiation, suspended monocytic cells become adherent, increasing the expression of adhesion molecules and leading to heterogeneous cell morphology with round, oval, or spherical shapes or with a spread membrane, stellate shapes, or ameboid shapes(Tsuchiya et al. 1982; Spano, Barni, and Sciola 2013; Starr et al. 2018; Gordon, Plüddemann, and Martinez Estrada 2014). The expression of integrin CD11b is especially abundant in the podosomes of THP-1 PMA differentiated macrophages(Hirvonen et al. 2020; Clercq et al. 2013). This integrin binds to multiple extracellular matrix (ECM) and vascular proteins, like fibrinogen and ICAM-1, and is commonly used as a marker for macrophage differentiation(Lamers, Plüss, and Ricklin 2021; Sándor et al. 2016; Khan, Khan, and Gupta 2018). CD11b is also known to be a therapeutic target for other diseases like Lupus, and various types of cancer and has been used as a prognosis marker in myeloid leukemia(Khan, Khan, and Gupta 2018; Maiguel et al. 2011; Geraghty et al. 2020; Ibrahim et al. 2018; Faridi et al. 2017). Importantly, CD11b regulates macrophage polarization(Schmid et al. 2018).

Macrophage migration and phagocytic activity require adhesion molecules and the cytoskeleton to polarize towards the infection site. Integrins group around podosomes(Tian et al. 2019; Hirvonen et al. 2020; Clercq et al. 2013), structures used by the cell to migrate and strongly adhere and which are directly linked to the cell cytoskeleton dynamics(Ehrlicher et

al. 2011; Sun, Guo, and Fässler 2016; Proag et al. 2015). The state of the cell cytoskeleton directly modulates cell mechanics, cell shape and proportionate anchors for cell adhesion(Keeling et al. 2017; Xiaoli Zhang et al. 2020; Pegoraro, Janmey, and Weitz 2017; Rigato et al. 2015). It has also been shown that adhesion structures are important for the development of stress fibers, cytoskeletal force transmission and cell shape(Katoh, Kano, and Ookawara 2008; Gupta et al. 2016; Elosegui-Artola et al. 2016; Schwarz and Gardel 2012). Furthermore, it has been shown that leukocytes react to the stiffness of the substrate, for example, neutrophils display a spread morphology and become stiffer on stiff substrates and monocytes differentiate differently according to the substrate viscoelastic properties(Roca-Cusachs et al. 2006; Vining et al. 2022). Moreover, monocyte firm adhesion to epithelial cells is mediated by integrins(Xiaohui Zhang et al. 2004) and monocyte adhesion is modulated by cell mechanics(Rico et al. 2010). Previous studies have shown that, in the early stages (minutes) of the differentiation process, monocytes soften, increasing their adhesion capacity(Wojcikiewicz et al. 2003) and that inflammatory response is sensitive to physical changes in the substrate(McWhorter et al. 2013). Moreover, the mechanical properties of macrophages are involved in their activation state(Patel et al. 2012), and cell mechanics allow distinguishing between pro-inflammatory (M1) and anti-inflammatory (M2) macrophages under inflammatory conditions(Evers et al., n.d.; Court, Malier, and Millet 2019). Finally, during phagocytosis, macrophages stiffen, increase membrane and cortical tension, exert high traction forces and change the organization of the cytoskeleton(Irmscher et al. 2013; Kovari et al. 2016; Lam et al. 2009). Thus, cell mechanics and cell adhesion play an interconnected role in the physiological state of the leukocytes during the inflammatory response and are of vital importance in macrophage physiology. However, little is known about how adhesion and mechanics are related in fully differentiated macrophages. Therefore, it is important to measure cell mechanics and cell adhesion at the same time during the monocyte's differentiation into macrophages.

Atomic force microscopy (AFM) is a robust technique providing highly quantitative data that allows the mechanical characterization of soft biological samples with nanometer resolution(Rico, Wojocikiewicz, and Moy 2008; Rico et al. 2005). Coupling AFM with other optical techniques has been reported on several occasions(Trache and Meininger 2005; C. M. Franz and Puech 2008; Cascione et al. 2017). For example, AFM for cell mechanics is commonly coupled to an inverted optical microscope for precise tip positioning over the sample. This gives access to using other techniques like immunofluorescence, confocal, total internal reflection fluorescence (TIRF) or stimulated emission depletion (STED) microscopy(Janel et al. 2017; Vickery and Dunn 2001; Becerra et al. 2021; Clemens M. Franz and Müller 2005; Curry et al. 2017). Interference contrast microscopy (ICM) imaging provides a measure of the distance of the cell's membrane to the glass surface with nanometric precision and in a millisecond time scale, which makes it suitable to study adhesion in living cells(Kovari et al. 2016; Limozin and Sengupta 2009; Daniel Axelrod 2001; D Axelrod 1981; Curtis 1964; Weber 2003; Dejardin et al. 2018). Therefore, coupling AFM with ICM will allow to simultaneously determine viscoelasticity and adhesion on living cells.

While biological and biochemical characterization of macrophage differentiation has been extensively studied, here, we propose a biophysical approach based on viscoelasticity and adhesion providing a novel, mechanical point of view. For this purpose, we correlated AFM, ICM and holographic tomography to quantify morphological, viscoelastic and adhesion properties during the process of macrophage differentiation. AFM mechanical mapping

coupled to ICM allows to simultaneously determine cell viscoelasticity (apparent Young's modulus and fluidity) and adhesion area (Figure 1 a). The THP-1 monocytic cell line stimulated with phorbol 12-myristate 13-acetate (PMA) is a widely used and robust model of macrophage differentiation(Tsuchiya et al. 1982; Park et al. 2007). While it has b , its genetic and monocyte differentiated macrophages proteomic expression is considered valid for simple differentiation and polarization studies [Tedesco 2018] THP-1 PMA differntiated macrophages We first characterized cell morphology changes with label-free holographic tomography images, obtaining 3D holographic reconstructions of the cells(Cotte et al. 2013), and used flow cytometry to quantify the evolution of CD11b expression, a macrophage marker. This allowed initial characterization and quantitative classification of morphological populations. Differentiated M0 macrophages increased their volume and showed two populations: spread and round. Viscoelastic maps showed that monocytes stiffened and solidified upon differentiation into macrophages. Stiffening and solidification correlated with larger adhesion areas as quantified by ICM. However, when adhesion molecules were cleaved and cells detached, resuspended macrophages remained stiffer and more solid-like than monocytes, suggesting permanent cytoskeleton reorganization.

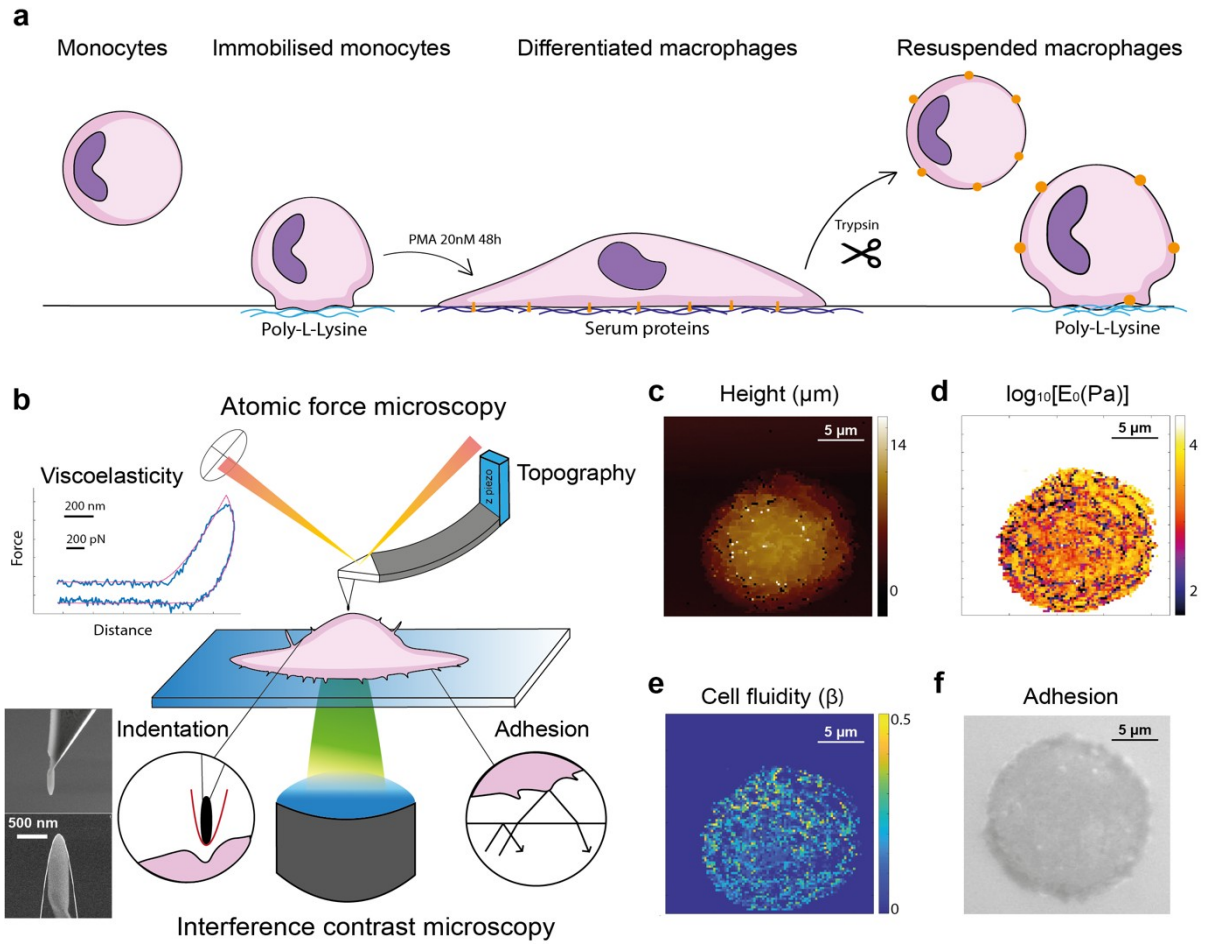

Figure 1. a. Experimental conditions to probe adhesion and viscoelasticity of monocytes and M0 macrophages. a. THP-1 cells (monocytes) were grown in suspension and immobilized on poly-L-lysine (PLL) coated glass. THP-1 cells treated with 20nM PMA differentiated into M0 macrophages after 48 hours and spontaneously adhered to the surface. Trypsin treatment

cleaves proteins, like integrins, detaching macrophages that were immediately immobilized on PLL-coated surfaces. b. Coupled system of atomic force microscopy (AFM) and interference contrast microscopy (ICM). Optical interferences and AFM force curves allowed the formation of adhesion images and mechanical maps, respectively. c. AFM mechanical mapping mode creates topography maps from the contact point detected in the force-indentation curves (inset in b). d. Apparent Young's modulus (E_0) and e. fluidity maps, were obtained from the viscoelastic fit (Eq. 1) to the force-indentation curves. f. Adhesion area of the very same cell obtained using ICM.

Results

CD11b expression

THP-1 cells were treated with PMA for 24, 48 and 72 hours (Supplementary Figure 1) and CD11b integrin cell surface expression was quantified over time using flow cytometry (Figure 2 a-b). PMA is known to induce the differentiation of THP-1 cells into M0 macrophages, indicated by the upregulated expression of integrin subunit CD11b (ITGAM gene, forming Mac-1 with CD18)(Tsuchiya et al. 1982; Schwende et al. 1996; Spano, Barni, and Sciola 2013; Starr et al. 2018). In agreement with previous reports, CD11b expression increased with time, reaching maximum levels after 48 hours of PMA treatment, and maintaining a similar level for 72 hours(Starr et al. 2018). In addit
on, from the forward and sid
e scatter signals, the cellular granularity or co
reported by other works
[Deigneaultt 2010] (Supplementary fi
Thus, at 48h THP-1 cells were considered as differentiated into M0 macrophages. PMA concentrations of 20 nM, 50 nM, 100 nM, and 200 nM were also tested obtaining similar results (Supplementary Figure 2). Thus, the minimum concentration needed for CD11b expression was used to induce differentiation, 20nM.

Tomography imaging of cell membranes

To assess the morphological changes during THP-1 differentiation, individual cells were imaged by laser holographic tomography at 48h after 20nM PMA stimulation. This label-free *in vivo* technique generates 3D stacks and visualizes changes in refractive index throughout samples and is particularly suited for highlighting cellular membranes (Figure 2 c-f). At 48h, M0 macrophages presented two phenotypes: 1) a prevalent round morphology (Figure 2 d), and 2) a spread morphology with roughly circular areas on the substrate (Figure 2 e). Similar changes in morphology have been identified before as a signature of differentiation. We, therefore, analyzed both morphological phenotypes separately and used image analysis to quantify the volume, surface area and compactness of the cells before and after differentiation (Figure 2 g-i). Differentiated macrophages displayed lower compactness, larger volume, and larger surface area than monocytes. The spread phenotype had the lowest compactness, as expected given the less spherical shape, and the largest volume and surface area (both ~2.6 times larger than monocytes). In addition, tomography imaging revealed that all differentiated macrophages contained more and larger cytoplasmic vesicles(Tsuchiya et al. 1982; Daigneault et al. 2010). To assess the effect of substrate adhesion on cell morphology, macrophages were resuspended using trypsin, immobilized on PLL-coated bottom dishes and immediately imaged. Trypsin was used to unspecifically digest most adhesion molecules from the cell surface as a control in nanomechanical maps. Resuspended cells did not spread and presented reduced volume and surface area and slightly higher compactness than the round phenotype (Figure 2 g-i). Therefore, this technique allowed us to classify cells into four states: monocytes, round and spread macrophages and resuspended macrophages.

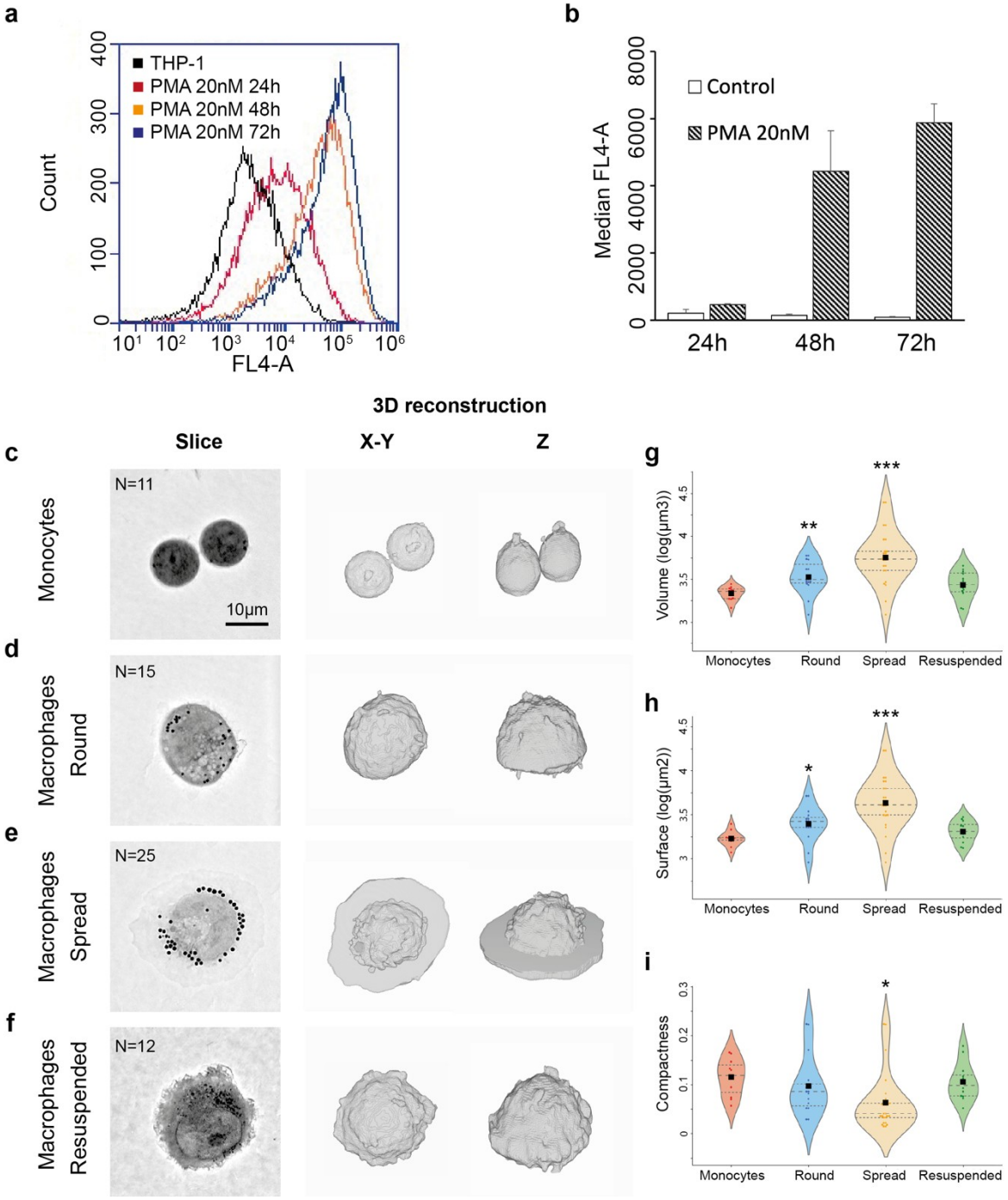

Figure 2. Molecular and morphological characterization of monocytes and macrophages. a-b Flow cytometry. a. Fluorescence intensity (FI) of CD11b obtained by flow cytometry on THP-1 cells after 20nM PMA treatment at times 24h, 48h and 72h and control. b. CD11b mean +/- standard deviation of median FI (MFI) values from three flow cytometry experiments at 24h, 48h, 72h, for 20nM PMA treated cells and control. c-i. Holographic tomography images of control and 20mM PMA treated THP-1 cells (48h). c-f. Image slices close to the substrate and 3D image reconstructions (from 96 slices) for monocytes, round, spread and resuspended macrophages. Internal vesicles were visible as dark spots in the slices, but filtered out for the cell membrane 3D reconstruction. g-i. Volume, surface and compactness were determined after 3D single-cell reconstruction of tomographic images of monocytes and round, spread and resuspended macrophages (11, 15, 25, and 12 cells, respectively. Squares are mean, dashed lines are median, dotted lines 25% and 75% quartiles.

).* = p<0.05, ** = p<0.01, ***=p<0.001

Mechanical properties and topography

To determine how the viscoelasticity changed among the different groups described, AFM was used to obtain mechanical maps on individual cells (30x30µm with 64x64 pixels, 468 nm/pixel), containing 4096 force-distance curves. The apparent Young's modulus (E_0) and the cell fluidity (β) were determined by fitting a parabolic viscoelastic contact model to each force-indentation curve (Equation 1). Thus, maps revealed topography, apparent YM and cell fluidity (Figure 3 a-c). Topography was extracted from the contact point determined by the fit, reflecting the undeformed cell surface. Topography maps allowed us to discern between the different cell morphologies, spread macrophages showing a spread membrane of ~400 nm thickness (Figure 3 a)

figure 3). Average roughness values did not change importantly across cell phenotypes and provided measurements although R_q was slightly lower and less dispersed in monocytes and spread macrophages.

From apparent YM (E_0) maps, macrophages appeared to be on average stiffer than monocytes, regardless of the cell state. Apparent YM (E_0) maps allowed us to assess the distribution of stiffnesses across the cell (Figure 3 b). On spread macrophages, the membrane extension appeared to be ~10-fold stiffer than the body of the cell. Also shown in Figure 3 b, the body center of round and spread macrophages was stiffer than the body periphery, while the values were more homogeneous in resuspended macrophages. Protrusions and microvilli appeared to be stiffer than the average body. Histograms of $\log(E_0)$ pooling all maps were generated, further evidencing the differences between cell states (Figure 3 d). Monocytes showed a distribution of $\log[E_0]$ values with mean±SD of 2.38±0.63 log[Pa] (~240 Pa). For macrophages, the mean±SD appeared at 3.08±0.69 log[Pa] (~1200 Pa) (round) and 3.43±0.73 log[Pa] (~2691 Pa) (spread). Interestingly, spread macrophages presented a histogram with clear two peaks, at 3.4 log[Pa] (~2511 Pa) and 4.2 log[Pa] (~15 kPa), corresponding to the cell body and the spread regions, respectively, as observed in the mechanical maps (Figure 3 b). Interestingly, resuspended macrophages showed a mean±SD of 3.20±0.61 log[Pa] (~1580 Pa), slightly stiffer than round macrophages.

To notice, β values very close to zero were frequent as show the

b]

, reflecting a perfectly elastic response.

In all states, a linear trend was observed between β and $\log[E_0]$ (Figure 3 f). However, from monocytes to macrophages, the peak was shifted towards lower β and higher $\log[E_0]$. In the case of spread macrophages, two clear populations were observed, corresponding to the body and spread areas (Figure 3 f).

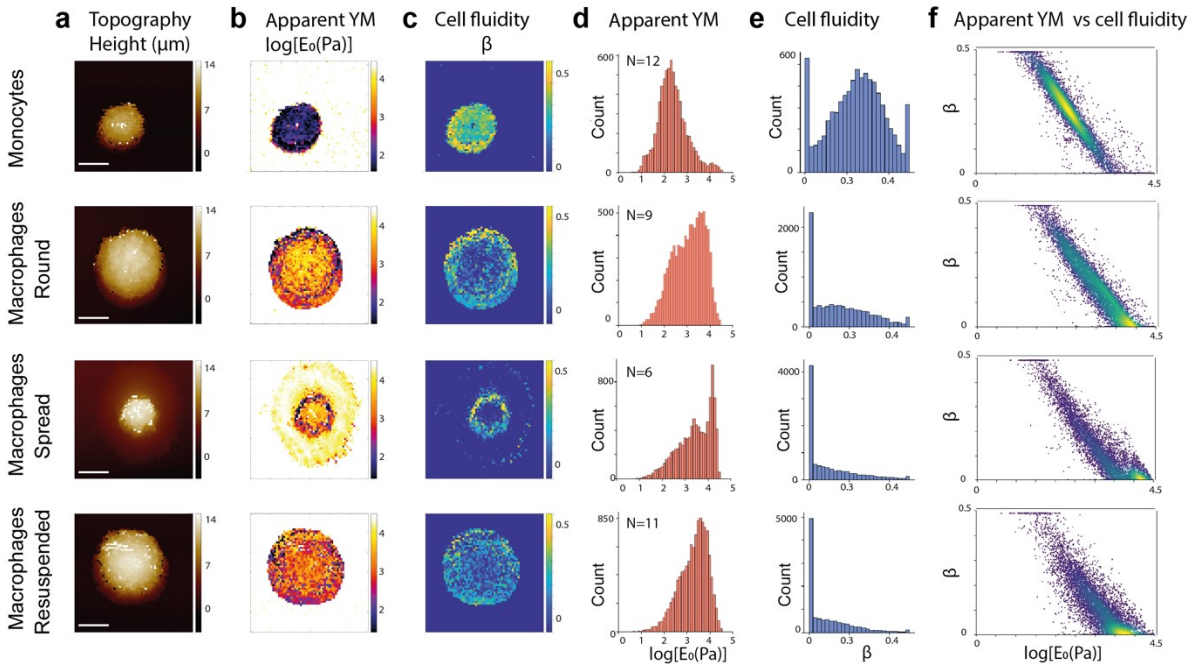

Figure 3. Atomic force microscopy topography and viscoelastic maps. 30x30 µm, 64x64 px, 4096 F-d curves per map at 468 nm/pixel. a. Topographical maps extracted from the contact point of the F-d curves (scale bar 10µm). b. Apparent YM maps (E_0), color scale: 1.7-4.47 log[Pa], with saturated values on the glass surface. c. Cell fluidity maps (β), color scale: 0-0.5. d. Apparent YM (E_0) distribution in log scale. Monocytes E_0 peak (~240 Pa), macrophages round E_0 peak (~1200 Pa, p<0.001 ***), macrophages spread E_0 peak(~2691 Pa, p<0.001 ***), macrophages resuspended E_0 peak(~1580 Pa, p<0.001 ***). e. Cell fluidity (β) histogram. Monocytes β peak (0.24), macrophages round β peak (0.15, p<0.001 ***), macrophages spread β peak (0.09, p<0.001 ***), macrophages resuspended β peak (0.08, p<0.001 ***). f. Cell fluidity (β) versus log[E_0]. Monocytes N=12, round macrophages N=9, spread macrophages N=6, resuspended macrophages N=11. The number of curves for d-f was between 8000 and 10000 per condition studied after filtering out the background curves.

Cell adhesion by ICM

The coupled AFM/ICM system allowed to directly quantify the adhesion of cells to the substrate (Figure 4) on the very same cells mapped by AFM. This allowed direct correlation between adhesion and viscoelastic parameters. The ICM image pixels values are related to the distance between the cell membrane and the glass surface, following a damped sinusoidal relationship as the distance increases, with a wavelength of ~250 nm (half the wavelength of incident green light, λ, divided by the refraction index of the medium n=1.33 for water (Limozin and Sengupta 2009)). The periphery of cells was brighter than the cell center, while spread regions (thinner than $\lambda/2$) appeared darker. Darker regions (lower pixels values) have been shown to correlate to shorter distances between the membrane and the surface and tight contact structures, such as focal adhesion plaques, and are usually interpreted as adhesion domains and as denser cytoskeleton regions (Curtis 1964; Drazba et al. 1997; Holt et al. 2008). In THP-1 cells, it has been shown that cells showing dark contact resist better to flow removal(Pierres et al. 2003). Therefore, pixel values provide a semi-quantitative measure of cell adhesion strength and of cytoskeleton rich structures. The ICM images were processed as explained in the methods and the distribution of pixels values from the cell area was plotted as averaged histograms (Supplementary figure Figure 7 d-g). Macrophages appeared darker than monocytes, suggesting that macrophages of any state had stronger adhesion compared to monocytes. In addition, ICM images on macrophages often show small, circular dark areas,

resembling podosome-like structures, and circular ruffles suggesting actin bundles, as observed before(Spano, Barni, and Sciola 2013; Tian et al. 2019; Hirvonen et al. 2020). Resuspended macrophages appeared lighteı with punctual strong adhesion areas.

ICM images were processed as described in the methods to quantify the adhesion area (μm^2), perimeter (µm), ellipse major/minor ratio, and compactness (Figure 4 e-g). Macrophages showed larger adhesion area than monocytes, especially in the spread phenotype (4 and 6-fold larger for round and spread, respectively), recovering monocyte values when resuspended (Figure 4 e), in accordance with tomographic imaging results for surface and volume (Figure 2 g-h). The perimeter followed the same but less pronounced trend (Figure 4 f). The ratio between the ellipse major and minor diameters showed that spread macrophages had rounder adhesion areas (Figure 4 g).

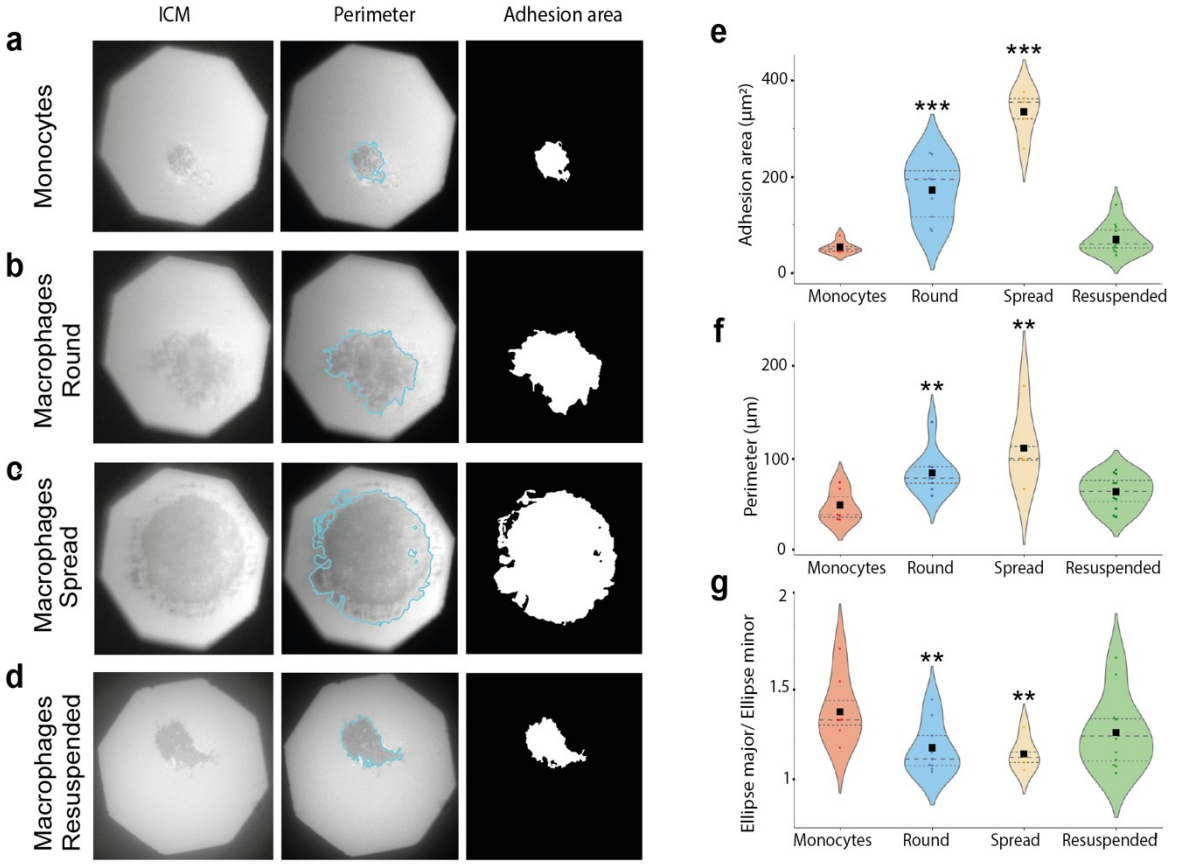

centeı

h. intensity profiles

p-values from t-tests against monocytes are shown as *=p<0.05, **=p<0.01, and ***=p<0.001.

maintaining the solid-like behavior of spread macrophages with the apparent Young's modulus of round macrophages.

Discussion

Tomography imaging revealed the cell surface, without labeling and with nanometric resolution (183 nm in xy, 312 nm in z), while 3D reconstruction allowed us to determine the morphology of cells, providing a quantitative measure of the different cell phenotypes (Figure 2 g-i). Compared to monocytes, differentiated macrophages, regardless of the condition, increased volume and surface, and reduced compactness. As reported before, macrophages often presented round phenotypes and, less frequently, membrane spreading (Figure 2 d and e, respectively)(Tsuchiya et al. 1982; Spano, Barni, and Sciola 2013). We named these two populations round and spread macrophages. This first visual division corresponds to a 1.7-fold increase in surface and volume and a 1.5-fold decrease in compactness of spread macrophages compared to round ones. Resuspended macrophages presented similar compactness, and slightly smaller volume and surface than round macrophages (Figure 2 g-i). Therefore, tomography imaging allows the establishment of cell populations based on quantitative morphological features of unlabeled cells *in-vivo*. Recent work on blood samples from COVID-19 patients revealed increased size and volume of monocytes (~1.2-fold) due to dysregulated inflammatory response or cytokine storm syndrome(Kubánková et al. 2021), which, according to our quantification, may be an early signature of differentiation. In this direction, blood samples from COVID-19 patients have also reported monocytes expressing macrophage markers like CD80 and CD206(D. Zhang et al. 2021).

Tomography imaging also allows visualization of internal membranes, such as vesicles (Figure 2 c-f). THP-1 cells after differentiation showed an increased number of small, dark spheres, resembling vesicles, characteristic of macrophages(Daigneault et al. 2010). Lysosomal vesicles are related to the antimicrobial activity of macrophages and their content is released in case of pathogenicity. In the resuspended phenotype, the number of vesicles diminished, suggesting release during resuspension, which may explain the reduced volume and surface area. Therefore, vesicle number may be used as an additional quantitative marker of monocyte differentiation.

AFM and ICM were combined to simultaneously obtain topography, viscoelasticity and adhesion maps on the very same cells. This coupling approach has been used before to characterize hyaluronan brushes and living cells(Trache and Meininger 2005; Attili and Richter 2012), but not to correlate adhesion and mechanics on cells. A possible improvement of the current setup would involve adding a lambda quarter waveplate between the objective and the sample and using different illumination wavelengths. This would help increase the signal-to-noise ratio and allow direct quantification of the substrate-membrane distance(Limozin and Sengupta 2009; Dejardin et al. 2018).

To obtain mechanical maps of living monocytes and macrophages, we used long and relatively sharp AFM tips. Long tips of ~20 μm were necessary to allow mapping of 10-14 μm height cells without touching the cell body with the cantilever arm. Moreover, long tips allowed us to obtain force curves at a relatively high velocity (~200 μm/s) with minimal contribution of the substrate to viscous drag forces on the cantilever(Alcaraz et al. 2002) (supplementary Figure 9). The increase in the viscous drag coefficient (b) of a cantilever near a wall is well known and has been reported before(Alcaraz et al. 2002; Rigato et al. 2017;

Janovjak, Struckmeier, and Müller 2005). The choice of PFQNM-LC probes was made keeping in mind this behavior. Indeed, these probes feature a remarkably large tip (~20 µm, Supplementary Figure 10) which provides a large gap between the cantilever base and the surface, minimizing the increased viscous drag near the surface compared to cantilevers with shorter tips. The change in *b* factor difference between the top of the cell and the spread area is <25%. This is the area most affected by the near surface, only present in spread macrophages. Within the other cell types, the change in *b* across the cell surface is <5%. Therefore, this variation did not considerably influence our results. To show this, we analyzed the spread macrophage shown in Figure 3 with two values of *b* (0.7 and 0.9 pN·s/µm, 25% change). The results are shown in Supplementary figure 9 and reflect minimal variation between the two maps. Therefore, we decided to use the value of *b* near the nuclear region to avoid overcorrecting the viscous drag effect.

The relatively sharp tips used (~30 nm) provide high-resolution maps, revealing the structure and mechanics of the cell surface with submicrometer resolution. While we were able to obtain good quality maps on living cells at 234 nm/pixel (Figure 1), the long time acquisition (30 min) limited the viability of the cells and thus, we opted to acquire maps at lower resolution (468 nm/pixel) but higher acquisition rate (~7 min per map). Nevertheless, the maps allowed visualization of subcellular structures, such as filopodia, and quantified their mechanical properties (Figure 3), without apparent cell perturbation. This was important to detect the contribution of cell stiffness and fluidity of the different regions across the cell surface.

Compared to monocytes, maps revealed stiffening and solidification of macrophages in all states (E_0, Figure 3).

and sub-micrometer resolution. While previous works reported stiffening of whole cell in previous works)

Round macrophages (1202 Pa on average, β=0.15) were 5 times stiffer and considerably less viscous than monocytes (240 Pa, β=0.24). Remarkably, spread macrophages were ~10-fold stiffer than monocytes and even more solid-like than round macrophages (2691 Pa, β=0.09). This dramatic increase in E_0 was due to its bimodal distribution, corresponding to the cell body and spread area, with peaks at 2511 Pa and 15 kPa, respectively. The first peak of the apparent YM distribution corresponded to the cell body, slightly stiffer than that of round macrophages, being this region less viscous, suggesting that the spreading may induce tension or prestress in the cell cortex(Lee, Herant, and Heinrich 2011; Cordes et al. 2020). The second peak of the YM distribution correlated with the spread region and was ~60 times stiffer than monocytes and almost perfectly elastic (β~0). The thickness of the spread region was between ~200 nm and ~2000 nm, while the thickness of the nuclear and perinuclear regions ranged between 5 and 14 µm (Supplementary Figure 8). The possible influence of the bottom substrate was corrected based on the model developed by Chadwick (see methods) (Dimitriadis et al. 2002). Given the low magnitude of the tip radius (~30 nm) and the relatively low indentation over the spread region (<200 nm), the average correction was <30%. The correction across the nuclear and perinuclear regions was <2%. Therefore, spread regions were remarkably stiffer and almost perfectly solid-like. This may be important for phagocytic activity.

Our results show that protruding structures such as microvilli (small protrusions across the cell body) and lamellipodia (spread regions) were stiffer and more solid-like, likely due to enrichment of cytoskeletal structures (Supplementary figure 14) and adhesion molecules(Spano, Barni, and Sciola 2013). Indeed, immunostaining of Spreading has been shown to involve modulation of the membrane tension, which increases once the membrane area is depleted(Gauthier et al. 2011). While we believe that the membrane tension is not probed by the AFM in our measurements (being the underlying cytoskeleton much stiffer than the fluid membrane), membrane area depletion is known to lead to activation of actomyosin contraction, which may increase the prestress in the cytoskeleton and, thus, the scaling modulus(Schierbaum, Rheinlaender, and Schäffer 2019).

Quantification of surface roughness did not change signific

Interestingly, microvilli and lamellipodia appeared stiff and almost purely solid ($\beta \sim 0$). Macrophages are highly mechanosensitive cells(Liu et al. 2016; Patel et al. 2012; El-Kirat-Chatel and Dufrêne 2012; Meli et al. 2019; Maruyama, Nemoto, and Yamada 2019; McWhorter, Davis, and Liu 2015), a more solid-like response of lamellipodia and the apical part of microvilli may result in higher mechanosensitivity and more efficient downstream transmission of the mechanical stresses. Thus, we conclude that monocytes differentiate into macrophages by developing highly mechanosensitive, solid-like regions, lamellipodia (membrane spreading) and microvilli and protrusions (nuclear and perinuclear regions). These solidified structures may render mechanosensing more efficient, minimizing the dissipation of energy due to viscous effects. A similar purely elastic response has been recently reported on thin periphery regions of various adherent cell lines(Mandriota et al. 2019), suggesting solidification as a possible fingerprint of mechanosensing during cell spreading and migration.

Spread macrophages extended the membrane, modulating both cell stiffness and adhesion to the substrate, resembling what has been termed frustrated phagocytosis(Spano, Barni, and Sciola 2013; Kovari et al. 2016). As previously reported, contact activated neutrophils on stiff surfaces changed to a spread morphology with a stiffer and more solid-like mechanical response, while monocytes differentiate aberrantly on stiff substrates(Roca-Cusachs et al. 2006; Vining et al. 2022). The stiffening of leukocytes during inflammation has been reported and hypothesized to be a fingerprint of leukocyte activation, inducing adhesion and extravasation(Kubánková et al. 2021; Preira et al. 2015; Worthen et al. 1989). It has also been described that macrophage activation state in M1 or M2 phenotypes change their mechanical properties(Patel et al. 2012; Meli et al. 2019). In apparent contradiction, THP-1 cells treated with PMA have been reported to soften in the short term (~30min), enhancing cell adhesion(Wojcikiewicz et al. 2003). In contrast, after long-term stimulation (48h), we observed stiffer macrophages, likely due to cytoskeleton reorganization, accumulation of actin filaments in the cell edge and podosome formation(Spano, Barni, and Sciola 2013; Tian et al. 2019; Hirvonen et al. 2020). This suggests that PMA-induced short-time softening (minutes) helps monocytes to adhere to the substrate, consequently inducing cytoskeleton remodeling, stiffening and solidification at longer times. These changes may allow macrophages to migrate and phagocyte external agents more efficiently(Tsuchiya et al. 1982; Chang et al. 2012; Starr et al. 2018). Interestingly, when macrophage adhesion was suppressed through trypsinization, macrophages still remained 6.6-fold stiffer (1585 Pa) than monocytes, probably due to a permanent reorganization of the cytoskeleton, likely of actin, and associated proteins(Clercq et al. 2013; Herdoiza Padilla et al. 2019). Taken together, these

results suggest that macrophage stiffening is due both to cell adhesion-mediated tension and cytoskeleton remodeling.

While surface roughness did not sig

In addition, the adhesion areas appeared to be more circular for macrophages (Figure 4 g).

These cha

as reported before(Kurihara et al 2011) and suggested by

the darker

Figure 4h and

Supplementary figure 7 d-g). Given that CD11b (훼M expression increases dramatically at 48h, it seems reasonable that the stronger and larger adhesion was mediated substantially by integrin Mac-1, formed by subunits CD11b and CD18, likely binding to serum proteins like fibrinogen adsorbed to the glass surface(Spano, Barni, and Sciola 2013; Starr et al. 2018; Gordon, Plüddemann, and Martinez Estrada 2014). However, other integrins (휶5 CD49e, 휶V

1 CD29, 훽2 CD18 and 훽 3 CD61) also

increase the expression levels in THP-1

differentiatec macrophages and may mediate this binding, particularly 훽V훽3 (

Kurihara et al 2011).

When macrophages were resuspended, the adhesion perimeter and area

returned to monocyte levels.

ICM intensity values also returned to monocyte levels, except for a sı

Some ICM images

of macrophages only

presented darker spots (Supplementary figure 6), which c

(Spano, Barni, and Sciola 2013; Tian et al. 2019; Hirvonen et al. 2020; Curtis 196

The relationship between adhesion and mechanics in macrophages has been suggested before. The adhesiveness of THP-1 cells to various ligands has been measured by optical tweezers, showing an increase in binding forces after 48h PMA differentiation that correlated with higher traction forces exerted by cells(Z. L. Zhou et al. 2016). In addition, stiffening of the extracellular matrix due to crosslinking increased adhesiveness in THP-1 PMA-differentiated cells(Hsieh et al. 2019). Quantification of the apparent Young's modulus, fluidity and adhesion area on the very same cells allowed us to directly compare the average parameters against each other. Overall, monocyte differentiation revealed a correlation between adhesion and viscoelastic parameters (Figure 5 a-b). Monocytes differentiated into macrophages stiffened, solidified, and showed larger adhesion area. However, within populations, larger adhesion did not always result in stiffer and more solid-like cells. This is clearly observed in spread macrophages, in which even a negative correlation of $\log[E_0]$ vs adhesion is observed (Figure 5 a). Thus, changes in cell mechanics may be triggered by integrin expression, as suggested recently on melanoma cells(Lacaria et al. 2020), and then reinforced during the initial steps of firm adhesion. After this, a possible mechanical upper bound may limit the relationship between adhesion expansion and stiffness, as suggested on phagocytic neutrophils(Zak et al. 2022). In accordance, when adhesion was suppressed in resuspended macrophages, the viscoelastic parameter values did not recover monocyte levels (Figure 5 a-b). This suggests that adhesion, stiffening and solidification progress together during differentiation but that may become independent of each other once differentiation is reached.

It is interesting to notice that, on average, monocytes, round and spread macrophages all fell within the same trend line of β vs $\log[E_0]$, while resuspended macrophages slightly deviated from this trend. Interestingly, using the three main parameters as dimensions of a phase

space, we observed that the four cell phenotypes clustered around different regions (Figure 5 d).

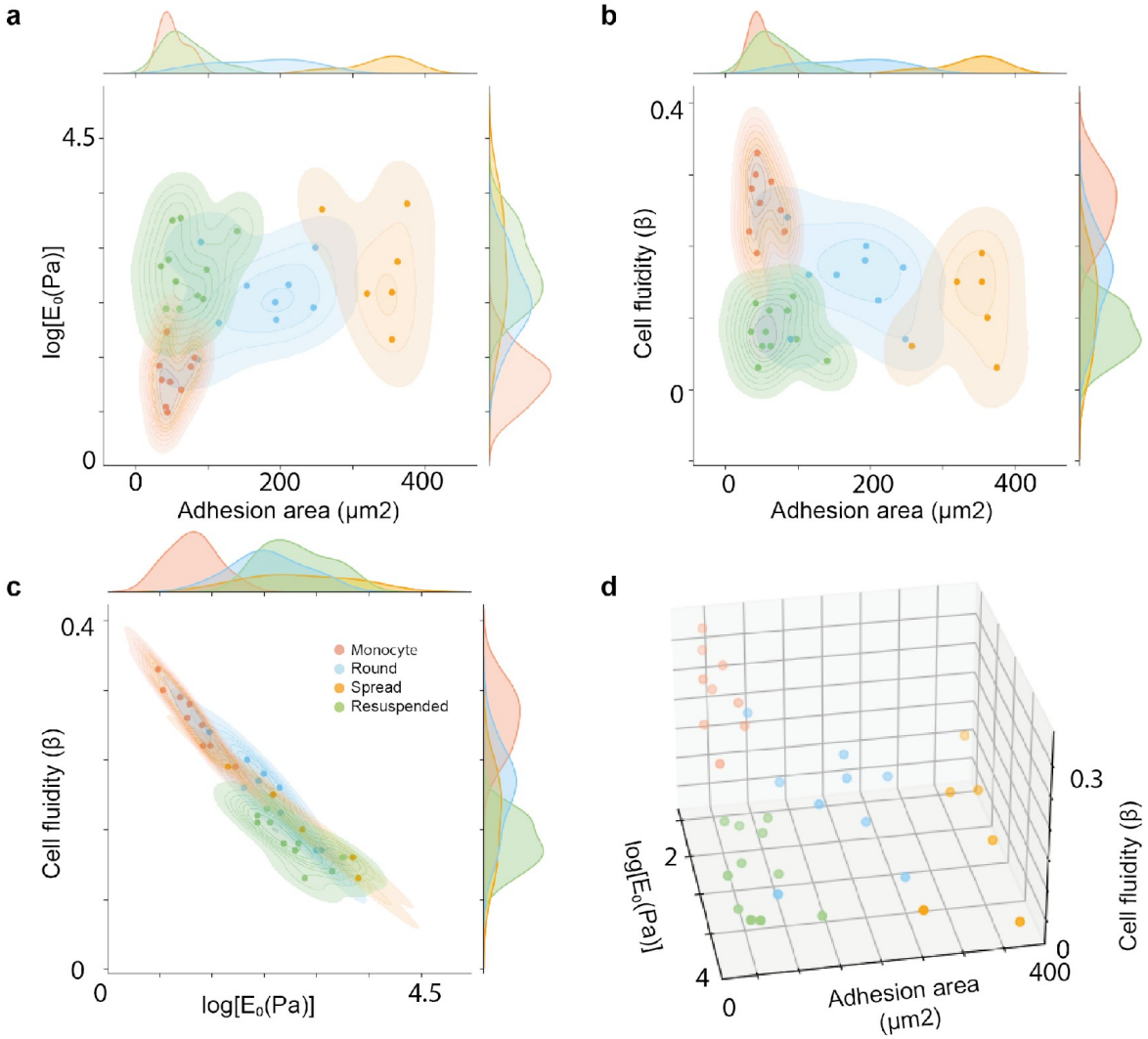

Figure 5. Viscoelasticity and cell adhesion area comparison for single cell analysis (each symbol corresponding to a single cell). a. Apparent YM ($Log_{10}[E_0]$) versus adhesion area (μm^2). b. Cell fluidity (β) versus adhesion area (μm^2). c. Cell fluidity (β) versus apparent YM ($Log_{10}[E_0]$). d. Cell fluidity (β), apparent YM ($Log_{10}[E_0]$) and adhesion area. Different colors correspond to different cell conditions.

The correlation between adhesion and viscoelasticity and the increased expression of CD11b may suggest that integrin expression may be the triggering factor to induce stiffening and solidification. Nevertheless, mechanical hallmarks of macrophages remained independent of adhesion once differentiation was reached, as shown on resuspended macrophages ' suggest ' CD11b expression has been reported as a key biomarker in immune cells for the progression of diseases like cancer and autoimmunity(Khan, Khan, and Gupta 2018; Fagerholm et al. 2013; Saed et al. 2018; Ibrahim et al. 2018; Faridi et al. 2017; S. Xu et al. 2015; Schmid et al. 2018), our results suggest that viscoelasticity and adhesion of immune cells may emerge also as relevant biomarker(Maiguel et al. 2011; Lekka et al. 1999; 2001; Guck et al. 2005; W. Xu et al. 2012; Júnior et al. 2021; Rosenbluth, Lam, and Fletcher 2006; Samouillan et al. 2020; Martinez-Vidal et al. 2021; Gurkan 2021; K. N. Zhou et al. 2020).

Conclusions

In conclusion, we applied holographic tomography imaging as a quantitative, non-invasive and label-free technique uncovering round and spread macrophage phenotypes with larger volume and surface area than monocytes. Coupling of AFM mechanical mapping with ICM allowed us to quantify the adhesion and viscoelasticity on the very same cells revealing viscoelastic hallmarks of monocyte differentiation into macrophages that correlated with adhesion area. Compared to monocytes, macrophages showed larger adhesion area, higher apparent YM (E_0) and decreased cell fluidity (β), particularly in lamellipodia and microvilli. Mechanical changes may be a consequence of adhesion to the surface through a reinforcement mechanism, as shown in the spread macrophages whose population stiffening almost tripled compared to the round phenotype, mainly due to the spread regions. However, this correlation fails within spread macrophages when using average cell values. Recent work has reported stiffening and solidification of neutrophils and macrophages during phagocytosis(Zak et al. 2022), which might be frustrated in the spreading phenotype(Kovari et al. 2016). Taken together, our results support the idea that stiffening, solidification and size change of monocytes during differentiation into macrophages are biologically important. We propose that larger, stiffer, and solidified macrophages may be more efficient during mechanosensitive activities, such as migration and phagocytosis(Evans, Leung, and Zhelev 1993; Masters et al. 2013).

Methods

Cell culture

The THP-1 cell line was obtained from ATCC (American Type Culture Collection, TIB-202) and cultured in RPMI-1640 media (Gibco, Thermofisher, Ref.11875093) supplemented with 1% sodium pyruvate (Gibco, Thermofisher, Ref. 11360070), 1% of MEM NEAA (Gibco, Thermofisher, Ref. 10370047), 1% Penicillin-streptomycin (Gibco, Thermofisher, Ref. 15140148), HEPES 10mM (Gibco, Thermofisher, Ref.15630080) and 10% fetal bovine serum (FBS). Cells were maintained at 37ºC, 5% CO2 and 95% humidity. The cells were kept between a concentration of 2-8 x 10^5 cells/mL, splitting them every 2-3 days. Cells were discarded after 20 passages to avoid any drifting in the phenotype. All % values are v/v %. Cells were routinely tested for mycoplasma contamination.

Cell differentiation

THP-1 cells were cultured in the cell culture media described before with 20nM phorbol 12-myristate 13-acetate (PMA) (Sigma Aldrich, Ref. P1585) for 48h in glass-bottom Petri dishes. After 48h the cells were washed once with fresh cell culture media, without PMA, prewarmed at 37ºC.

Atomic force microscopy measurements

Cultured cells' viscoelastic properties and topography were measured with AFM-force mapping mode in a Nanowizard 4 (Bruker-JPK) using pre-calibrated PFQNM-LC-cal cantilevers (Bruker). The force set point was set at 0.8 nN, speed at 200 µm/s and the range at 15µm in Z. The first experiments were conducted at high resolution (234 nm/px) and then the resolution was set to 64x64 px in a 30 µm square area (468 nm/px). For the monocyte and macrophage measurements, the cells in suspension were immobilized with a poly-L-lysin 0.01% solution coating of high molecular weight (>80kDa), (Sigma Aldrich Ref.25988-63-0). For the adhesion control, THP-1 differentiated cells were trypsinized for 3-5 minutes at 37ºC, centrifuged at 1200 rpm for 10 min and seeded with fresh culture media without PMA in a glass-bottom petri dish coated with poly-L-lysine. The measurements of all conditions

were taken in the culture media without PMA, at room temperature and 20 mM Hepes in a window of time of 2 hours at room temperature.

The inverse of the optical lever sensitivity (invOLS) was calibrated using the SNAP approach from the thermal spectra in liquid(Schillers et al. 2017). For that, we used the pre-calibrated spring constant of the cantilevers and the correction factors described in Rodríguez-Ramos(Rodriguez-Ramos and Rico 2021).

The viscous drag coefficient of the cantilever (b=0.7 pN·s/μm) was determined as the difference between approach and retract forces before contact from force curves obtained on top of the cells.

The geometry and dimensions of the cantilever tip were determined from scanning electron microscopy images. Briefly, a paraboloid was fitted to the last 500 nm of the protrusion present at the apex of the pyramidal tip (Fig. 1 and Supplementary figure 10). The effective radius was determined to 30 nm.

Viscoelastic model

The apparent Young's modulus (E_0) and cell fluidity (β) were determined by simultaneously fitting the approach and retract curves to a viscoelastic contact model assuming a paraboloid of equivalent radius (R) indenting a viscoelastic sample following power law rheology of time-dependent Young's modulus $E(t)=E_0(t/t_0)^{\beta}$ (Efremov et al. 2017), [Lacaria 2022 in preparation]. The model is based on the approach proposed before for a paraboloid but with different approach and retract indentation velocities(Brückner, Nöding, and Janshoff 2017; Sanchez et al. 2021). The approach and retract force versus time traces ($F_a(t)$ and $F_r(t)$, respectively) were:

$$F_a(t) = \frac{4}{3}\frac{E_0}{1-\nu^2}\sqrt{R}\, {v_a}^{\frac{3}{2}} \frac{{t_0}^{\beta} 3\sqrt{\pi}\Gamma(1-\beta)}{4\Gamma\left(\frac{5}{2}-\beta\right)}\, t^{\frac{3}{2}-\beta}$$

$$F_r(t) = \frac{4}{3}\frac{E_0}{1-\nu^2}\sqrt{R}\, v_a^{3/2}\left(\frac{t}{t_0}\right)^{-\beta} t_1^{3/2}\, {}_2F_1\left(\frac{3}{2},\beta;\frac{5}{2};\frac{t_1}{t}\right) \quad (1)$$

[Lacaria 2022 in preparation] where ${}_2F_1$ is the ordinary hypergeometric function, Γ is the gamma funciton, ν=0.5 is the Possion ratio, v_a and v_t are the approach and retract velocities, respectively, t_0=1s and t_1 is the time point from the retract curve at which the area of contact equals the area of contact of the approach and is found to be

$$t_1 = t - \left(1+\frac{v_r}{v_a}\right)^{1/(1-\beta)}(t-t_m)$$

where t_m is the time at maximum indentation. The viscous drag force was added to the approach and retract curves from the viscous drag factor times the velocity calculated at each time point: $b\cdot v_a(t)$ and $-b\cdot v_r(t)$, respectively.

The maps of spread macrophages were corrected for the bottom effect using the model developed by Chadwick for a thin layer of thickness h bonded to the substrate(Dimitriadis et al. 2002). The correction factor used was

$$BEC = 1 + 1.133\,\chi + 1.283\,\chi^2 + 0.769\,\chi^3 + 0.0975\,\chi^4$$

$$\chi = \frac{\sqrt{\square}}{\square}$$

Force curve c

Topography maps and roughness calculation

AFM topography maps were reconstructed from the point of contact dete

5µm X 5µm

, fitting a paraboloid to flatten the surfa

before AFM maps

Schneider, Rasband, and Eliceiri 2012; 'TAPAS: Towards Automated Processing and Analysis of Multi-Dimensional Bioimage Data - PMC' n.d.).

From these param

Two distinct cell regions were extracted separately: one corresponding to the high contrast central part of the cell, and the remaining part corresponding to thin membrane extensions at the cell perimeter. The central cell region was detected using a classical segmentation protocol. For that, stacks were filtered with a 3D median filter with radii 4x4x2, followed by automatic thresholding (using the triangle algorithm) and a "fill holes" procedure. The weakly-contrasted thin membrane boundaries were manually delineated. Finally, the individual values computed for the central and peripheral regions were combined to obtain total single cell volume and surface areas.

Flow cytometry

Immunocytochemistry
THP-1 monocytes were immobilized on glass cover slides following the directly fixated, permeabilized, and stained described in the mentioned protocol. The concentrations following stains were used: actin CellMask Green (Invitrogen Ref.A57243 using Zeiss confocal microscope (LSM880) with an objective Plan-Apochromat 63X/1.4 OI.

Statistics

Differences in the parameters obtained from the holograp 훼

, and ICM imaging (perimeter, adhesion area, an

-tests of per-cell average values against the control condition (monocytes) of . *p*

sterisks in the figures as *

Acknowledgments
FR thanks Andreas Janshoff for useful insights on the viscoelastic model. The project was supported by the European Union's Horizon 2020 research and innovation programmes No 812772 (project Phys2BioMed, Marie Skłodowska-Curie grant), the Japanese Society for Promotion of Science (JSPS) short-term fellowship, the European Research Council (ERC) under the European Union's Horizon 2020 research and innovation programme (grant agreement No 772257), the ATIP Avenir with financial support from ITMO Cancer of Aviesan on funds Cancer 2021 administered by Inserm, and the Japanese Ministry of Education, Culture, Sports, Science and Technology (World Premier International Research Center Initiative (WPI). The project leading to this publication has received funding from France 2030, the French Government program managed by the French National Research Agency (ANR-16-CONV-0001) and from Excellence Initiative of Aix-Marseille University - A*MIDEX. We thank Dr Millet and his laboratory for providing the low-passage THP-1 cells from ATCC (American Type Culture Collection, TIB-202). Electron microscopy experiments were carried out at the PICsL-FBI core electron microscopy facility (Nicolas Brouilly, IBDM, AMU-Marseille UMR 7288), a member of the national infrastructure France-BioImaging supported by the French National Research Agency (ANR-10-INBS-0004).

Author contributions

ME designed and performed all experiments, results interpretation and manuscript writing.

. CV

BIBLIOGRAPHY

Alcaraz, J., L. Buscemi, M. Puig-de-Morales, J. Colchero, A. Baró, and D. Navajas. 2002. 'Correction of Microrheological Measurements of Soft Samples with Atomic Force Microscopy for the Hydrodynamic Drag on the Cantilever'. *Langmuir* 18 (3): 716–21. https://doi.org/10.1021/la0110850.

Attili, Seetharamaiah, and Ralf P. Richter. 2012. 'Combining Colloidal Probe Atomic Force and Reflection Interference Contrast Microscopy to Study the Compressive Mechanics of Hyaluronan Brushes'. *Langmuir* 28 (6): 3206–16. https://doi.org/10.1021/la204602n.

Auwerx, J. 1991. 'The Human Leukemia Cell Line, THP-1: A Multifacetted Model for the Study of Monocyte-Macrophage Differentiation'. *Experientia* 47 (1): 22–31. https://doi.org/10.1007/BF02041244.

Axelrod, D. 1981. 'Cell-Substrate Contacts Illuminated by Total Internal Reflection Fluorescence.' *Journal of Cell Biology* 89 (1): 141–45. https://doi.org/10.1083/jcb.89.1.141.

Axelrod, Daniel. 2001. 'Total Internal Reflection Fluorescence Microscopy in Cell Biology'. *Traffic* 2 (11): 764–74. https://doi.org/10.1034/j.1600-0854.2001.21104.x.

Becerra, Natalia, Barbara Salis, Mariateresa Tedesco, Susana Moreno Flores, Pasquale Vena, and Roberto Raiteri. 2021. 'AFM and Fluorescence Microscopy of Single Cells with Simultaneous Mechanical Stimulation via Electrically Stretchable Substrates'. *Materials (Basel, Switzerland)* 14 (15): 4131. https://doi.org/10.3390/ma14154131.

Brückner, Bastian Rouven, Helen Nöding, and Andreas Janshoff. 2017. 'Viscoelastic Properties of Confluent MDCK II Cells Obtained from Force Cycle Experiments'. *Biophysical Journal* 112 (4): 724–35. https://doi.org/10.1016/j.bpj.2016.12.032.

Cascione, Mariafrancesca, Valeria de Matteis, Rosaria Rinaldi, and Stefano Leporatti. 2017. 'Atomic Force Microscopy Combined with Optical Microscopy for Cells Investigation'. *Microscopy Research and Technique* 80 (1): 109–23. https://doi.org/10.1002/jemt.22696.

Chang, Mei-Ying, Duen-Yi Huang, Feng-Ming Ho, Kuo-Chin Huang, and Wan-Wan Lin. 2012. 'PKC-Dependent Human Monocyte Adhesion Requires AMPK and Syk Activation'. Edited by Jeffrey K. Harrison. *PLoS ONE* 7 (7): e40999. https://doi.org/10.1371/journal.pone.0040999.

Clercq, Sarah De, Ciska Boucherie, Joël Vandekerckhove, Jan Gettemans, and Aude Guillabert. 2013. 'L-Plastin Nanobodies Perturb Matrix Degradation, Podosome Formation, Stability and Lifetime in THP-1 Macrophages'. *PLOS ONE* 8 (11): e78108. https://doi.org/10.1371/journal.pone.0078108.

Cordes, Andrea, Hannes Witt, Aina Gallemí-Pérez, Bastian Brückner, Florian Grimm, Marian Vache, Tabea Oswald, et al. 2020. 'Prestress and Area Compressibility of Actin Cortices Determine the Viscoelastic Response of Living Cells'. *Physical Review Letters* 125 (6): 068101. https://doi.org/10.1103/PhysRevLett.125.068101.

Cotte, Yann, Fatih Toy, Pascal Jourdain, Nicolas Pavillon, Daniel Boss, Pierre Magistretti, Pierre Marquet, and Christian Depeursinge. 2013. 'Marker-Free Phase Nanoscopy'. *Nature Photonics* 7 (2): 113–17. https://doi.org/10.1038/nphoton.2012.329.

Court, Magali, Marie Malier, and Arnaud Millet. 2019. '3D Type I Collagen Environment Leads up to a Reassessment of the Classification of Human Macrophage Polarizations'. *Biomaterials* 208 (July): 98–109. https://doi.org/10.1016/j.biomaterials.2019.04.018.

Curry, Nathan, Grégory Ghézali, Gabriele S. Kaminski Schierle, Nathalie Rouach, and Clemens F. Kaminski. 2017. 'Correlative STED and Atomic Force Microscopy on Live Astrocytes Reveals Plasticity of Cytoskeletal Structure and Membrane Physical Properties during Polarized Migration'. *Frontiers in Cellular Neuroscience* 11. https://www.frontiersin.org/articles/10.3389/fncel.2017.00104.

Curtis, A. S. G. 1964. 'THE MECHANISM OF ADHESION OF CELLS TO GLASS'. *Journal of Cell Biology* 20 (2): 199–215. https://doi.org/10.1083/jcb.20.2.199.

Daigneault, Marc, Julie A. Preston, Helen M. Marriott, Moira K. B. Whyte, and David H. Dockrell. 2010. 'The Identification of Markers of Macrophage Differentiation in PMA-Stimulated THP-1 Cells and Monocyte-Derived Macrophages'. *PLOS ONE* 5 (1): e8668. https://doi.org/10.1371/journal.pone.0008668.

Dejardin, Marie-Julie, Arnaud Hemmerle, Anaïs Sadoun, Yannick Hamon, Pierre-Henri Puech, Kheya Sengupta, and Laurent Limozin. 2018. 'Lamellipod Reconstruction by Three-Dimensional Reflection Interference Contrast Nanoscopy (3D-RICN)'. *Nano Letters* 18 (10): 6544–50. https://doi.org/10.1021/acs.nanolett.8b03134.

Dimitriadis, Emilios K., Ferenc Horkay, Julia Maresca, Bechara Kachar, and Richard S. Chadwick. 2002. 'Determination of Elastic Moduli of Thin Layers of Soft Material Using the Atomic Force Microscope'. *Biophysical Journal* 82 (5): 2798–2810. https://doi.org/10.1016/S0006-3495(02)75620-8.

Drazba, Judith, Patricia Liljelund, Carolyn Smith, Ross Payne, and Vance Lemmon. 1997. 'Growth Cone Interactions with Purified Cell and Substrate Adhesion Molecules Visualized by Interference Reflection Microscopy'. *Developmental Brain Research* 100 (2): 183–97. https://doi.org/10.1016/S0165-3806(97)00041-2.

Efremov, Yuri M., Wen-Horng Wang, Shana D. Hardy, Robert L. Geahlen, and Arvind Raman. 2017. 'Measuring Nanoscale Viscoelastic Parameters of Cells Directly from AFM Force-Displacement Curves'. *Scientific Reports* 7 (1): 1541. https://doi.org/10.1038/s41598-017-01784-3.

Ehrlicher, A. J., F. Nakamura, J. H. Hartwig, D. A. Weitz, and T. P. Stossel. 2011. 'Mechanical Strain in Actin Networks Regulates FilGAP and Integrin Binding to Filamin A'. *Nature* 478 (7368): 260–63. https://doi.org/10.1038/nature10430.

El-Kirat-Chatel, Sofiane, and Yves F. Dufrêne. 2012. 'Nanoscale Imaging of the Candida–Macrophage Interaction Using Correlated Fluorescence-Atomic Force Microscopy'. *ACS Nano* 6 (12): 10792–99. https://doi.org/10.1021/nn304116f.

Elosegui-Artola, Alberto, Roger Oria, Yunfeng Chen, Anita Kosmalska, Carlos Pérez-González, Natalia Castro, Cheng Zhu, Xavier Trepat, and Pere Roca-Cusachs. 2016. 'Mechanical Regulation of a Molecular Clutch Defines Force Transmission and Transduction in Response to Matrix Rigidity'. *Nature Cell Biology* 18 (5): 540–48. https://doi.org/10.1038/ncb3336.

Evans, E, A Leung, and D Zhelev. 1993. 'Synchrony of Cell Spreading and Contraction Force as Phagocytes Engulf Large Pathogens'. *Journal of Cell Biology* 122 (6): 1295–1300. https://doi.org/10.1083/jcb.122.6.1295.

Evers, Tom M. J., Vahid Sheikhhassani, Huaqi Tang, Mariëlle C. Haks, Tom H. M. Ottenhoff, and Alireza Mashaghi. n.d. 'Single-Cell Mechanical Characterization of Human Macrophages'. *Advanced NanoBiomed Research* n/a (n/a): 2100133. https://doi.org/10.1002/anbr.202100133.

Fagerholm, SC, M MacPherson, MJ James, C Sevier-Guy, and CS Lau. 2013. 'The CD11b-Integrin (ITGAM) and Systemic Lupus Erythematosus'. *Lupus* 22 (7): 657–63. https://doi.org/10.1177/0961203313491851.

Faridi, Mohd Hafeez, Samia Q. Khan, Wenpu Zhao, Ha Won Lee, Mehmet M. Altintas, Kun Zhang, Vinay Kumar, et al. 2017. 'CD11b Activation Suppresses TLR-Dependent Inflammation and Autoimmunity in Systemic Lupus Erythematosus'. *The Journal of Clinical Investigation* 127 (4): 1271–83. https://doi.org/10.1172/JCI88442.

Fougerolles, Antonin R. de, Gloria Chi-Rosso, Adriana Bajardi, Philip Gotwals, Cynthia D. Green, and Victor E. Koteliansky. 2000. 'Global Expression Analysis of Extracellular Matrix–Integrin Interactions in Monocytes'. *Immunity* 13 (6): 749–58. https://doi.org/10.1016/S1074-7613(00)00073-X.

Franz, C. M., and P.-H. Puech. 2008. 'Atomic Force Microscopy: A Versatile Tool for Studying Cell Morphology, Adhesion and Mechanics'. *Cellular and Molecular Bioengineering* 1 (4): 289–300. https://doi.org/10.1007/s12195-008-0037-3.

Franz, Clemens M., and Daniel J. Müller. 2005. 'Analyzing Focal Adhesion Structure by Atomic Force Microscopy'. *Journal of Cell Science* 118 (22): 5315–23. https://doi.org/10.1242/jcs.02653.

Gauthier, Nils C., Marc Antoine Fardin, Pere Roca-Cusachs, and Michael P. Sheetz. 2011. 'Temporary Increase in Plasma Membrane Tension Coordinates the Activation of Exocytosis and Contraction during Cell Spreading'. *Proceedings of the National Academy of Sciences* 108 (35): 14467–72. https://doi.org/10.1073/pnas.1105845108.

Geraghty, Terese, Anugraha Rajagopalan, Rabail Aslam, Alexander Pohlman, Ishwarya Venkatesh, Andrew Zloza, David Cimbaluk, David G. DeNardo, and Vineet Gupta. 2020. 'Positive Allosteric Modulation of CD11b as a Novel Therapeutic Strategy Against Lung Cancer'. *Frontiers in Oncology* 10. https://www.frontiersin.org/articles/10.3389/fonc.2020.00748.

Gordon, Siamon, Annette Plüddemann, and Fernando Martinez Estrada. 2014. 'Macrophage Heterogeneity in Tissues: Phenotypic Diversity and Functions'. *Immunological Reviews* 262 (1): 36–55. https://doi.org/10.1111/imr.12223.

Guck, Jochen, Stefan Schinkinger, Bryan Lincoln, Falk Wottawah, Susanne Ebert, Maren Romeyke, Dominik Lenz, et al. 2005. 'Optical Deformability as an Inherent Cell Marker for Testing Malignant Transformation and Metastatic Competence'. *Biophysical Journal* 88 (5): 3689–98. https://doi.org/10.1529/biophysj.104.045476.

Gupta, Mukund, Bryant Doss, Chwee Teck Lim, Raphael Voituriez, and Benoit Ladoux. 2016. 'Single Cell Rigidity Sensing: A Complex Relationship between Focal Adhesion Dynamics and Large-Scale Actin Cytoskeleton Remodeling'. *Cell Adhesion & Migration* 10 (5): 554–67. https://doi.org/10.1080/19336918.2016.1173800.

Gurkan, Umut A. 2021. 'Biophysical and Rheological Biomarkers of Red Blood Cell Physiology and Pathophysiology'. *Current Opinion in Hematology* 28 (3): 138–49. https://doi.org/10.1097/MOH.0000000000000639.

Herdoiza Padilla, Estefania, Peter Crauwels, Tim Bergner, Nicole Wiederspohn, Sabrina Förstner, Rebecca Rinas, Anna Ruf, et al. 2019. 'Mir-124-5p Regulates Phagocytosis of Human Macrophages by Targeting the Actin Cytoskeleton via the ARP2/3 Complex'. *Frontiers in Immunology* 10. https://www.frontiersin.org/articles/10.3389/fimmu.2019.02210.

Hirvonen, Liisa M., Richard J. Marsh, Gareth E. Jones, and Susan Cox. 2020. 'Combined AFM and Super-Resolution Localisation Microscopy: Investigating the Structure and Dynamics of Podosomes'. *European Journal of Cell Biology* 99 (7): 151106. https://doi.org/10.1016/j.ejcb.2020.151106.

Holt, M.r., Y. Calle, D.h. Sutton, D.r. Critchley, G.e. Jones, and G.a. Dunn. 2008. 'Quantifying Cell–Matrix Adhesion Dynamics in Living Cells Using Interference Reflection Microscopy'. *Journal of Microscopy* 232 (1): 73–81. https://doi.org/10.1111/j.1365-2818.2008.02069.x.

Homma, Y., C. B. Henning-Chubb, and E. Huberman. 1986. 'Translocation of Protein Kinase C in Human Leukemia Cells Susceptible or Resistant to Differentiation Induced by Phorbol 12-Myristate 13-Acetate.' *Proceedings of the National Academy of Sciences* 83 (19): 7316–19. https://doi.org/10.1073/pnas.83.19.7316.

Hsieh, Jessica Y., Mark T. Keating, Tim D. Smith, Vijaykumar S. Meli, Elliot L. Botvinick, and Wendy F. Liu. 2019. 'Matrix Crosslinking Enhances Macrophage Adhesion, Migration, and Inflammatory Activation'. *APL Bioengineering* 3 (1): 016103. https://doi.org/10.1063/1.5067301.

Ibrahim, Abeer, Asmaa M Zahran, Sanaa Shaker Aly, Ahmed Refaat, and Mohammed H Hassan. 2018. 'CD56 and CD11b Positivity with Low Smac/DIABLO Expression as Predictors of Chemoresistance in Acute Myeloid Leukaemia: Flow Cytometric Analysis'. *Asian Pacific Journal of Cancer Prevention : APJCP* 19 (11): 3187–92. https://doi.org/10.31557/APJCP.2018.19.11.3187.

Irmscher, Matthias, Arthur M. de Jong, Holger Kress, and Menno W. J. Prins. 2013. 'A Method for Time-Resolved Measurements of the Mechanics of Phagocytic Cups'. *Journal of The Royal Society Interface* 10 (82): 20121048. https://doi.org/10.1098/rsif.2012.1048.

Jain, Nikhil, Jens Moeller, and Viola Vogel. 2019. 'Mechanobiology of Macrophages: How Physical Factors Coregulate Macrophage Plasticity and Phagocytosis'. *Annual Review of Biomedical Engineering* 21 (1): 267–97. https://doi.org/10.1146/annurev-bioeng-062117-121224.

Janel, Sébastien, Elisabeth Werkmeister, Antonino Bongiovanni, Frank Lafont, and Nicolas Barois. 2017. 'Chapter 9 - CLAFEM: Correlative Light Atomic Force Electron Microscopy'. In *Methods in Cell Biology*, edited by Thomas Müller-Reichert and Paul Verkade, 140:165–85. Correlative Light and Electron Microscopy III. Academic Press. https://doi.org/10.1016/bs.mcb.2017.03.010.

Janovjak, Harald, Jens Struckmeier, and Daniel J. Müller. 2005. 'Hydrodynamic Effects in Fast AFM Single-Molecule Force Measurements'. *European Biophysics Journal* 34 (1): 91–96. https://doi.org/10.1007/s00249-004-0430-3.

Júnior, Constança, Maria Narciso, Esther Marhuenda, Isaac Almendros, Ramon Farré, Daniel Navajas, Jorge Otero, and Núria Gavara. 2021. 'Baseline Stiffness Modulates the Non-Linear Response to Stretch of the Extracellular Matrix in Pulmonary Fibrosis'. *International Journal of Molecular Sciences* 22 (23): 12928. https://doi.org/10.3390/ijms222312928.

Katoh, Kazuo, Yumiko Kano, and Shigeo Ookawara. 2008. 'Role of Stress Fibers and Focal Adhesions as a Mediator for Mechano-Signal Transduction in Endothelial Cells in Situ'. *Vascular Health and Risk Management* 4 (6): 1273–82.

Keeling, Michael C., Luis R. Flores, Asad H. Dodhy, Elizabeth R. Murray, and Núria Gavara. 2017. 'Actomyosin and Vimentin Cytoskeletal Networks Regulate Nuclear Shape, Mechanics and Chromatin Organization'. *Scientific Reports* 7 (1): 5219. https://doi.org/10.1038/s41598-017-05467-x.

Khan, Samia Q., Imran Khan, and Vineet Gupta. 2018. 'CD11b Activity Modulates Pathogenesis of Lupus Nephritis'. *Frontiers in Medicine* 5. https://www.frontiersin.org/article/10.3389/fmed.2018.00052.

Kohro, Takahide, Toshiya Tanaka, Takeshi Murakami, Yoichiro Wada, Hiroyuki Aburatani, Takao Hamakubo, and Tatsuhiko Kodama. 2004. 'A Comparison of Differences in the Gene Expression Profiles of Phorbol 12-Myristate 13-Acetate Differentiated THP-1 Cells and Human Monocyte-Derived Macrophage'. *Journal of Atherosclerosis and Thrombosis* 11 (2): 88–97. https://doi.org/10.5551/jat.11.88.

Kovari, Daniel T., Wenbin Wei, Patrick Chang, Jan-Simon Toro, Ruth Fogg Beach, Dwight Chambers, Karen Porter, Doyeon Koo, and Jennifer E. Curtis. 2016. 'Frustrated Phagocytic Spreading of J774A-1 Macrophages Ends in Myosin II-Dependent Contraction'. *Biophysical Journal* 111 (12): 2698–2710. https://doi.org/10.1016/j.bpj.2016.11.009.

Kubánková, Markéta, Bettina Hohberger, Jakob Hoffmanns, Julia Fürst, Martin Herrmann, Jochen Guck, and Martin Kräter. 2021. 'Physical Phenotype of Blood Cells Is Altered in COVID-19'. *BioRxiv*, February, 2021.02.12.429482. https://doi.org/10.1101/2021.02.12.429482.

Lacaria, Leda, Janina R. Lange, Wolfgang H. Goldmann, Felix Rico, and José Luis Alonso. 2020. 'Avβ3 Integrin Expression Increases Elasticity in Human Melanoma Cells'. *Biochemical and Biophysical Research Communications* 525 (4): 836–40. https://doi.org/10.1016/j.bbrc.2020.02.156.

Lam, Jonathan, Marc Herant, Micah Dembo, and Volkmar Heinrich. 2009. 'Baseline Mechanical Characterization of J774 Macrophages'. *Biophysical Journal* 96 (1): 248–54. https://doi.org/10.1529/biophysj.108.139154.

Lamers, Christina, Carla Johanna Plüss, and Daniel Ricklin. 2021. 'The Promiscuous Profile of Complement Receptor 3 in Ligand Binding, Immune Modulation, and Pathophysiology'. *Frontiers in Immunology* 12. https://www.frontiersin.org/article/10.3389/fimmu.2021.662164.

Lee, Cheng-Yuk, Marc Herant, and Volkmar Heinrich. 2011. 'Target-Specific Mechanics of Phagocytosis: Protrusive Neutrophil Response to Zymosan Differs from the Uptake of Antibody-Tagged Pathogens'. *Journal of Cell Science* 124 (7): 1106–14. https://doi.org/10.1242/jcs.078592.

Lekka, M., P. Laidler, D. Gil, J. Lekki, Z. Stachura, and A. Z. Hrynkiewicz. 1999. 'Elasticity of Normal and Cancerous Human Bladder Cells Studied by Scanning Force Microscopy'. *European Biophysics Journal* 28 (4): 312–16. https://doi.org/10.1007/s002490050213.

Lekka, M., Piotr Laidler, Jan Ignacak, M. \Labędź, J. Lekki, H. Struszczyk, Z. Stachura, and A. Z. Hrynkiewicz. 2001. 'The Effect of Chitosan on Stiffness and Glycolytic Activity of Human Bladder Cells'. *Biochimica et Biophysica Acta (BBA)-Molecular Cell Research* 1540 (2): 127–36.

Ley, Klaus, and Zhichao Fan. 2018. 'Leukocyte Adhesion'. In *Inflammation*, by Klaus Ley, 171–203. WORLD SCIENTIFIC. https://doi.org/10.1142/9789813109445_0005.

Limozin, Laurent, and Kheya Sengupta. 2009. 'Quantitative Reflection Interference Contrast Microscopy (RICM) in Soft Matter and Cell Adhesion'. *Chemphyschem: A European Journal of Chemical Physics and Physical Chemistry* 10 (16): 2752–68. https://doi.org/10.1002/cphc.200900601.

Liu, Chi, Chuan Wu, Qifen Yang, Jing Gao, Li Li, Deqin Yang, and Lingfei Luo. 2016. 'Macrophages Mediate the Repair of Brain Vascular Rupture through Direct Physical Adhesion and Mechanical Traction'. *Immunity* 44 (5): 1162–76. https://doi.org/10.1016/j.immuni.2016.03.008.

Maiguel, Dony, Mohd Hafeez Faridi, Changli Wei, Yoshihiro Kuwano, Keir M. Balla, Dayami Hernandez, Constantinos J. Barth, et al. 2011. 'Small Molecule–Mediated Activation of the Integrin CD11b/CD18 Reduces Inflammatory Disease'. *Science Signaling* 4 (189): ra57–ra57. https://doi.org/10.1126/scisignal.2001811.

Mandriota, Nicola, Claudia Friedsam, John A. Jones-Molina, Kathleen V. Tatem, Donald E. Ingber, and Ozgur Sahin. 2019. 'Cellular Nanoscale Stiffness Patterns Governed by Intracellular Forces'. *Nature Materials* 18 (10): 1071–77. https://doi.org/10.1038/s41563-019-0391-7.

Martinez-Vidal, Laura, Valentina Murdica, Chiara Venegoni, Filippo Pederzoli, Marco Bandini, Andrea Necchi, Andrea Salonia, and Massimo Alfano. 2021. 'Causal Contributors to Tissue Stiffness and Clinical Relevance in Urology'. *Communications Biology* 4 (1): 1011. https://doi.org/10.1038/s42003-021-02539-7.

Maruyama, Kentaro, Eiji Nemoto, and Satoru Yamada. 2019. 'Mechanical Regulation of Macrophage Function - Cyclic Tensile Force Inhibits NLRP3 Inflammasome-Dependent IL-1β Secretion in Murine Macrophages'. *Inflammation and Regeneration* 39 (1): 3. https://doi.org/10.1186/s41232-019-0092-2.

Masters, Thomas A., Bruno Pontes, Virgile Viasnoff, You Li, and Nils C. Gauthier. 2013. 'Plasma Membrane Tension Orchestrates Membrane Trafficking, Cytoskeletal Remodeling, and Biochemical Signaling during Phagocytosis'. *Proceedings of the National Academy of Sciences* 110 (29): 11875–80. https://doi.org/10.1073/pnas.1301766110.

McWhorter, Frances Y., Chase T. Davis, and Wendy F. Liu. 2015. 'Physical and Mechanical Regulation of Macrophage Phenotype and Function'. *Cellular and Molecular Life Sciences* 72 (7): 1303–16. https://doi.org/10.1007/s00018-014-1796-8.

McWhorter, Frances Y., Tingting Wang, Phoebe Nguyen, Thanh Chung, and Wendy F. Liu. 2013. 'Modulation of Macrophage Phenotype by Cell Shape'. *Proceedings of the National Academy of Sciences* 110 (43): 17253–58. https://doi.org/10.1073/pnas.1308887110.

Medzhitov, Ruslan. 2008. 'Origin and Physiological Roles of Inflammation'. *Nature* 454 (7203): 428–35. https://doi.org/10.1038/nature07201.

Meli, Vijaykumar S., Praveen K. Veerasubramanian, Hamza Atcha, Zachary Reitz, Timothy L. Downing, and Wendy F. Liu. 2019. 'Biophysical Regulation of Macrophages in Health and Disease'. *Journal of Leukocyte Biology* 106 (2): 283–99. https://doi.org/10.1002/JLB.MR0318-126R.

Muller, W. A. 2013. 'Getting Leukocytes to the Site of Inflammation'. *Veterinary Pathology* 50 (1): 7–22. https://doi.org/10.1177/0300985812469883.

Park, E. K., H. S. Jung, H. I. Yang, M. C. Yoo, C. Kim, and K. S. Kim. 2007. 'Optimized THP-1 Differentiation Is Required for the Detection of Responses to Weak Stimuli'. *Inflammation Research* 56 (1): 45–50. https://doi.org/10.1007/s00011-007-6115-5.

Patel, Naimish R., Medhavi Bole, Cheng Chen, Charles C. Hardin, Alvin T. Kho, Justin Mih, Linhong Deng, et al. 2012. 'Cell Elasticity Determines Macrophage Function'. *PLOS ONE* 7 (9): e41024. https://doi.org/10.1371/journal.pone.0041024.

Pegoraro, Adrian F., Paul Janmey, and David A. Weitz. 2017. 'Mechanical Properties of the Cytoskeleton and Cells'. *Cold Spring Harbor Perspectives in Biology* 9 (11): a022038. https://doi.org/10.1101/cshperspect.a022038.

Pierres, Anne, Philippe Eymeric, Emmanuelle Baloche, Dominique Touchard, Anne-Marie Benoliel, and Pierre Bongrand. 2003. 'Cell Membrane Alignment along Adhesive Surfaces: Contribution of Active and Passive Cell Processes'. *Biophysical Journal* 84 (3): 2058–70.

Preira, Pascal, Jean-Marie Forel, Philippe Robert, Paulin Nègre, Martine Biarnes-Pelicot, Francois Xeridat, Pierre Bongrand, Laurent Papazian, and Olivier Theodoly. 2015. 'The Leukocyte-Stiffening Property of Plasma in Early Acute Respiratory Distress Syndrome (ARDS) Revealed by a Microfluidic Single-Cell Study: The Role of Cytokines and Protection with Antibodies'. *Critical Care* 20 (1): 8. https://doi.org/10.1186/s13054-015-1157-5.

Proag, Amsha, Anaïs Bouissou, Thomas Mangeat, Raphaël Voituriez, Patrick Delobelle, Christophe Thibault, Christophe Vieu, Isabelle Maridonneau-Parini, and Renaud Poincloux. 2015. 'Working Together: Spatial Synchrony in the Force and Actin Dynamics of Podosome First Neighbors'. *ACS Nano* 9 (4): 3800–3813. https://doi.org/10.1021/nn506745r.

Rico, Félix, Calvin Chu, Midhat H. Abdulreda, Yujing Qin, and Vincent T. Moy. 2010. 'Temperature Modulation of Integrin-Mediated Cell Adhesion'. *Biophysical Journal* 99 (5): 1387–96. https://doi.org/10.1016/j.bpj.2010.06.037.

Rico, Félix, Pere Roca-Cusachs, Núria Gavara, Ramon Farré, Mar Rotger, and Daniel Navajas. 2005. 'Probing Mechanical Properties of Living Cells by Atomic Force Microscopy with Blunted Pyramidal Cantilever Tips'. *Physical Review E* 72 (2): 021914. https://doi.org/10.1103/PhysRevE.72.021914.

Rico, Félix, Ewa P. Wojocikiewicz, and Vincent T. Moy. 2008. 'Atomic Force Microscopy Studies of the Mechanical Properties of Living Cells'. In *Applied Scanning Probe Methods IX: Characterization*, edited by Masahiko Tomitori, Bharat Bhushan, and Harald Fuchs, 89–109. Nano Science and Technolgy. Berlin, Heidelberg: Springer. https://doi.org/10.1007/978-3-540-74083-4_4.

Rigato, Annafrancesca, Atsushi Miyagi, Simon Scheuring, and Felix Rico. 2017. 'High-Frequency Microrheology Reveals Cytoskeleton Dynamics in Living Cells'. *Nature Physics* 13 (8): 771–75. https://doi.org/10.1038/nphys4104.

Rigato, Annafrancesca, Felix Rico, Frédéric Eghiaian, Mathieu Piel, and Simon Scheuring. 2015. 'Atomic Force Microscopy Mechanical Mapping of Micropatterned Cells Shows Adhesion Geometry-Dependent Mechanical Response on Local and Global Scales'. *ACS Nano* 9 (6): 5846–56. https://doi.org/10.1021/acsnano.5b00430.

Roca-Cusachs, Pere, Isaac Almendros, Raimon Sunyer, Núria Gavara, Ramon Farré, and Daniel Navajas. 2006. 'Rheology of Passive and Adhesion-Activated Neutrophils Probed by Atomic Force Microscopy'. *Biophysical Journal* 91 (9): 3508–18. https://doi.org/10.1529/biophysj.106.088831.

Rodriguez-Ramos, Jorge, and Felix Rico. 2021. 'Determination of Calibration Parameters of Cantilevers of Arbitrary Shape by Finite Element Analysis'. *Review of Scientific Instruments* 92 (4): 045001. https://doi.org/10.1063/5.0036263.

Rosenbluth, Michael J., Wilbur A. Lam, and Daniel A. Fletcher. 2006. 'Force Microscopy of Nonadherent Cells: A Comparison of Leukemia Cell Deformability'. *Biophysical Journal* 90 (8): 2994–3003. https://doi.org/10.1529/biophysj.105.067496.

Rovera, Giovanni, Thomas G. O'Brien, and Leila Diamond. 1979. 'Induction of Differentiation in Human Promyelocytic Leukemia Cells by Tumor Promoters'. *Science* 204 (4395): 868–70. https://doi.org/10.1126/science.286421.

Saed, Ghassan M., Nicole M. Fletcher, Michael P. Diamond, Robert T. Morris, Nardhy Gomez-Lopez, and Ira Memaj. 2018. 'Novel Expression of CD11b in Epithelial Ovarian Cancer: Potential Therapeutic Target'. *Gynecologic Oncology* 148 (3): 567–75. https://doi.org/10.1016/j.ygyno.2017.12.018.

Samouillan, Valerie, Ignacio Miguel Martinez de Lejarza Samper, Aleyda Benitez Amaro, David Vilades, Jany Dandurand, Josefina Casas, Esther Jorge, et al. 2020. 'Biophysical and Lipidomic Biomarkers of Cardiac Remodeling Post-Myocardial Infarction in Humans'. *Biomolecules* 10 (11): 1471. https://doi.org/10.3390/biom10111471.

Sanchez, Juan G., Francisco M. Espinosa, Ruben Miguez, and Ricardo Garcia. 2021. 'The Viscoelasticity of Adherent Cells Follows a Single Power-Law with Distinct Local Variations within a Single Cell and across Cell Lines'. *Nanoscale* 13 (38): 16339–48. https://doi.org/10.1039/D1NR03894J.

Sándor, Noémi, Szilvia Lukácsi, Rita Ungai-Salánki, Norbert Orgován, Bálint Szabó, Róbert Horváth, Anna Erdei, and Zsuzsa Bajtay. 2016. 'CD11c/CD18 Dominates Adhesion of Human Monocytes, Macrophages and Dendritic Cells over CD11b/CD18'. *PLOS ONE* 11 (9): e0163120. https://doi.org/10.1371/journal.pone.0163120.

Schierbaum, Nicolas, Johannes Rheinlaender, and Tilman E. Schäffer. 2019. 'Combined Atomic Force Microscopy (AFM) and Traction Force Microscopy (TFM) Reveals a Correlation between Viscoelastic Material Properties and Contractile Prestress of Living Cells'. *Soft Matter* 15 (8): 1721–29. https://doi.org/10.1039/C8SM01585F.

Schillers, Hermann, Carmela Rianna, Jens Schäpe, Tomas Luque, Holger Doschke, Mike Wälte, Juan José Uriarte, et al. 2017. 'Standardized Nanomechanical Atomic Force Microscopy Procedure (SNAP) for Measuring Soft and Biological Samples'. *Scientific Reports* 7 (1): 5117. https://doi.org/10.1038/s41598-017-05383-0.

Schmid, Michael C., Samia Q. Khan, Megan M. Kaneda, Paulina Pathria, Ryan Shepard, Tiani L. Louis, Sudarshan Anand, et al. 2018. 'Integrin CD11b Activation Drives Anti-Tumor Innate Immunity'. *Nature Communications* 9 (1): 5379. https://doi.org/10.1038/s41467-018-07387-4.

Schneider, Caroline A., Wayne S. Rasband, and Kevin W. Eliceiri. 2012. 'NIH Image to ImageJ: 25 Years of Image Analysis'. *Nature Methods* 9 (7): 671–75. https://doi.org/10.1038/nmeth.2089.

Schwarz, Ulrich S., and Margaret L. Gardel. 2012. 'United We Stand – Integrating the Actin Cytoskeleton and Cell–Matrix Adhesions in Cellular Mechanotransduction'. *Journal of Cell Science* 125 (13): 3051–60. https://doi.org/10.1242/jcs.093716.

Schwende, Heike, Edith Fitzke, Petra Ambs, and Peter Dieter. 1996. 'Differences in the State of Differentiation of THP-1 Cells Induced by Phorbol Ester and 1,25-

Dihydroxyvitamin D $_3$'. *Journal of Leukocyte Biology* 59 (4): 555–61. https://doi.org/10.1002/jlb.59.4.555.
Spano, A., S. Barni, and L. Sciola. 2013. 'PMA Withdrawal in PMA-treated Monocytic THP-1 Cells and Subsequent Retinoic Acid Stimulation, Modulate Induction of Apoptosis and Appearance of Dendritic Cells'. *Cell Proliferation* 46 (3): 328–47. https://doi.org/10.1111/cpr.12030.
Starr, Tregei, Timothy J. Bauler, Preeti Malik-Kale, and Olivia Steele-Mortimer. 2018. 'The Phorbol 12-Myristate-13-Acetate Differentiation Protocol Is Critical to the Interaction of THP-1 Macrophages with Salmonella Typhimurium'. Edited by Dennis C. Ko. *PLOS ONE* 13 (3): e0193601. https://doi.org/10.1371/journal.pone.0193601.
Stone, William L., Hajira Basit, and Bracken Burns. 2022. 'Pathology, Inflammation'. In *StatPearls*. Treasure Island (FL): StatPearls Publishing. http://www.ncbi.nlm.nih.gov/books/NBK534820/.
Sun, Zhiqi, Shengzhen S. Guo, and Reinhard Fässler. 2016. 'Integrin-Mediated Mechanotransduction'. *Journal of Cell Biology* 215 (4): 445–56. https://doi.org/10.1083/jcb.201609037.
'TAPAS: Towards Automated Processing and Analysis of Multi-Dimensional Bioimage Data - PMC'. n.d. Accessed 25 November 2022. https://www.ncbi.nlm.nih.gov/pmc/articles/PMC8422341/.
Tian, Yongmei, Yongjun Wu, Lie Liu, Leiliang He, Jing Gao, Lulu Zhou, Fei Yu, Songcheng Yu, and Hongda Wang. 2019. 'The Structural Characteristics of Mononuclear-Macrophage Membrane Observed by Atomic Force Microscopy'. *Journal of Structural Biology* 206 (3): 314–21. https://doi.org/10.1016/j.jsb.2019.04.002.
Trache, Andreea, and Gerald A. Meininger. 2005. 'Atomic Force-Multi-Optical Imaging Integrated Microscope for Monitoring Molecular Dynamics in Live Cells'. *Journal of Biomedical Optics* 10 (6): 064023. https://doi.org/10.1117/1.2146963.
Tsuchiya, Shigeru, Yasuko Kobayashi, Yoichi Goto, Hidesada Okumura, Shingi Nakae, Tasuke Konno, and Keiya Tada. 1982. 'Induction of Maturation in Cultured Human Monocytic Leukemia Cells by a Phorbol Diester' 42: 7.
Van den Bossche, Jan, and Doina L. Saraber. 2018. 'Metabolic Regulation of Macrophages in Tissues'. *Cellular Immunology* 330 (August): 54–59. https://doi.org/10.1016/j.cellimm.2018.01.009.
Vicente-Manzanares, Miguel, and Francisco Sánchez-Madrid. 2004. 'Role of the Cytoskeleton during Leukocyte Responses'. *Nature Reviews Immunology* 4 (2): 110–22. https://doi.org/10.1038/nri1268.
Vickery, S. A., and R. C. Dunn. 2001. 'Combining AFM and FRET for High Resolution Fluorescence Microscopy'. *Journal of Microscopy* 202 (2): 408–12. https://doi.org/10.1046/j.1365-2818.2001.00857.x.
Vining, Kyle H., Anna E. Marneth, Kwasi Adu-Berchie, Joshua M. Grolman, Christina M. Tringides, Yutong Liu, Waihay J. Wong, et al. 2022. 'Mechanical Checkpoint Regulates Monocyte Differentiation in Fibrotic Niches'. *Nature Materials*, July, 1–12. https://doi.org/10.1038/s41563-022-01293-3.
Weber, Igor. 2003. '[2] Reflection Interference Contrast Microscopy'. In *Methods in Enzymology*, 361:34–47. Biophotonics, Part B. Academic Press. https://doi.org/10.1016/S0076-6879(03)61004-9.
Wojcikiewicz, E. P., X. Zhang, A. Chen, and V. T. Moy. 2003. 'Contributions of Molecular Binding Events and Cellular Compliance to the Modulation of Leukocyte Adhesion'. *Journal of Cell Science* 116 (June): 2531–39.
Worthen, G., B Schwab, E. Elson, and G. Downey. 1989. 'Mechanics of Stimulated Neutrophils: Cell Stiffening Induces Retention in Capillaries'. *Science* 245 (4914): 183–86. https://doi.org/10.1126/science.2749255.
Xu, Shuangnian, Xi Li, Jianmin Zhang, and Jieping Chen. 2015. 'Prognostic Value of CD11b Expression Level for Acute Myeloid Leukemia Patients: A Meta-Analysis'. *PLOS ONE* 10 (8): e0135981. https://doi.org/10.1371/journal.pone.0135981.

Xu, Wenwei, Roman Mezencev, Byungkyu Kim, Lijuan Wang, John McDonald, and Todd Sulchek. 2012. 'Cell Stiffness Is a Biomarker of the Metastatic Potential of Ovarian Cancer Cells'. *PLOS ONE* 7 (10): e46609. https://doi.org/10.1371/journal.pone.0046609.

Zak, Alexandra, Sophie Dupré-Crochet, Elodie Hudik, Avin Babataheri, Abdul I. Barakat, Oliver Nüsse, and Julien Husson. 2022. 'Distinct Timing of Neutrophil Spreading and Stiffening during Phagocytosis'. *Biophysical Journal* 121 (8): 1381–94. https://doi.org/10.1016/j.bpj.2022.03.021.

Zhang, Dan, Rui Guo, Lei Lei, Hongjuan Liu, Yawen Wang, Yili Wang, Hongbo Qian, et al. 2021. 'Frontline Science: COVID-19 Infection Induces Readily Detectable Morphologic and Inflammation-Related Phenotypic Changes in Peripheral Blood Monocytes'. *Journal of Leukocyte Biology* 109 (1): 13–22. https://doi.org/10.1002/JLB.4HI0720-470R.

Zhang, Xiaohui, Aileen Chen, Dina De Leon, Hong Li, Eisei Noiri, Vincent T. Moy, and Michael S. Goligorsky. 2004. 'Atomic Force Microscopy Measurement of Leukocyte-Endothelial Interaction'. *American Journal of Physiology-Heart and Circulatory Physiology* 286 (1): H359–67. https://doi.org/10.1152/ajpheart.00491.2003.

Zhang, Xiaoli, Luis R. Flores, Michael C. Keeling, Kristina Sliogeryte, and Núria Gavara. 2020. 'Ezrin Phosphorylation at T567 Modulates Cell Migration, Mechanical Properties, and Cytoskeletal Organization'. *International Journal of Molecular Sciences* 21 (2): 435. https://doi.org/10.3390/ijms21020435.

Zhou, Kevin Ning, Kuo-Tzu Sung, Chih-Hsuan Yen, Cheng-Huang Su, Ping-Ying Lee, Ta-Chuan Hung, Wen-Hung Huang, et al. 2020. 'Carotid Arterial Mechanics as Useful Biomarker of Extracellular Matrix Turnover and Preserved Ejection Fraction Heart Failure'. *ESC Heart Failure* 7 (4): 1615–25. https://doi.org/10.1002/ehf2.12714.

Zhou, Zhuo Long, Jing Ma, Ming-Hui Tong, Barbara Pui Chan, Alice Sze Tsai Wong, and Alfonso Hing Wan Ngan. 2016. 'Nanomechanical Measurement of Adhesion and Migration of Leukemia Cells with Phorbol 12-Myristate 13-Acetate Treatment'. *International Journal of Nanomedicine* Volume 11 (December): 6533–45. https://doi.org/10.2147/IJN.S118065.